國立臺灣大學理學院化學系

碩士論文

Department of Chemistry
College of Science
National Taiwan University
Master's Thesis

乙醯丙酮於溶劑中烯醇與酮的異構化反應動力學與機制

Kinetics and Mechanism of Enol-Keto Tautomerization of Acetylacetone in Solvents

羅冠杰

Guan-Jie Luo

指導教授：林志民 博士

Advisor: Jim Jr-Min Lin, Ph.D.

中華民國 114 年 8 月

August, 2025

doi:10.6342/NTU202503041

國立臺灣大學碩士學位論文
口試委員會審定書

NTU Master's Thesis
Oral Defense Approval Form

乙醯丙酮於溶劑中烯醇與酮的異構化反應動力學與機制

Kinetics and Mechanism of Enol-Keto Tautomerization of Acetylacetone in Solvents

本論文係羅冠杰君（學號 R10223173）在國立臺灣大學化學系完成之碩士學位論文，於民國 114 年 7 月 23 日承下列考試委員審查通過及口試及格，特此證明。

The student Guan-Jie Luo (student no. R10223173) enrolled in the Master Program of the Department of Chemistry, NTU has satisfactorily passed the oral defense on 2025/7/23 with the approval of all committee members as follows.

口試委員(Committee Members)：

（簽名 Signature）

（指導教授 Advisor）

系主任、所長 （簽章）

(Dept./Institute Chair's Signature and Seal)

doi:10.6342/NTU202503041

誌謝

本篇論文從做實驗到編寫完陸陸續續也花了一年多的時間，期間得到許多師長同儕的幫忙，陪我討論遇到的問題、改善實驗方法與編寫內容。首先當然要感謝我的指導教授－林志民老師，這幾年來教導我從化學上的知識到機械加工的技巧，連生活中處理事情的方法與態度都有談及，讓我受益良多。余慈顏老師也相當熱心協助我處理核磁共振儀器的實驗，本身已經夠忙了還來來回回載我去南港做實驗且實驗後遇到問題都不厭其煩的教導我，在此感謝您的熱忱教導。磊葳科技也提供桌上型核磁共振儀給我做實驗，時間也從原本借數個禮拜延到數個月，對此感到抱歉並感謝貴公司的幫忙。另外感謝姜昌明教授在時間上較晚詢問下，願意撥空擔任口試委員並給予許多論文上的改善建議。

從我進實驗室起美贊、明樂、妍秀就一直在各方面幫助我。美贊在我剛進來時指導我寫程式或練習處理儀器的數據，雖然後來去美國讀書沒有相處太久，但記憶深刻。明樂與妍秀則是數年來都一直協助我討論實驗、設計儀器、處理數據，平常也會隨便聊天，讓我生活更加充實有趣。後來遇到絜甯、彥儒、慶璿、宜睿也陪我處理實驗室大小事，生活上聊吃聊喝，豐富實驗室的時光，謝謝你們。實驗室期間內遇到的寒暑假專題生們太多人就不一一列舉，也為煩悶的生活增添不少色彩，謝謝。最後感謝原分所上的工廠師傅們幫我加工器具，行政助理們幫我處理報價單等各種事務，行政室與資訊室的人們協助我處理實驗室各種雜務，有你們才讓實驗室正常運作，謝謝。感謝一路走來所有幫助我完成學業的人。

doi:10.6342/NTU202503041

摘要

β-二羰基化合物，也稱為 1,3-二羰基化合物，在合成、配位化學及生物化學上有許多應用。乙醯丙酮 (AA) 為最簡單形式的 β-二羰基化合物，在不同溶劑中以各自的平衡常數與反應速率進行烯醇與酮式間的異構化反應。此實驗透過紫外線吸收光譜法與核磁共振探討 AA 在水、甲醇、乙醇、乙腈及它們的氘化溶劑中烯醇與酮式間異構化反應的動力學。實驗結果呈現 AA 的異構化反應在不涉及同位素交換時為一級反應動力學，且各溶劑中異構化速率為水 > 醇類 > 乙腈。此外在 CH_3CN 與醇類中，鹼催化效應分別為 269 及 1715 $s^{-1}\,M^{-1}$；酸催化效應僅在 CH_3CN 中較為顯著，且值比鹼催化效應弱，為 4.19 $s^{-1}\,M^{-1}$；在 CH_3CN 與醇類中，水催化效應分別為 1.69×10^{-4} 及 $1.51\times10^{-3}\,s^{-1}M^{-1}$。為了了解受同位素交換影響的偏離一級反應動力學的行為，我們分別在沒受鹼與受鹼催化的條件下提出動力學模型去模擬異構化反應中 AA 各形式的變化。模擬結果呈現 AA 異構化反應伴隨著同位素交換，且可透過溶劑形成的架橋與作為反應中間物的烯醇陰離子加速反應。此外，烯醇陰離子可以在沒有異構化反應下作同位素交換。最後 AA 於水及甲醇中異構化反應的動力學同位素效應 (kinetic isotope effect, KIE, k_H/k_D) 分別為 6.15 ± 0.39 與 6.35 ± 0.17。

關鍵字： 乙醯丙酮、異構化反應、反應動力學、紫外線吸收光譜法、核磁共振儀、動力學同位素效應

doi:10.6342/NTU202503041

ABSTRACT

β-diketones, also known as 1,3-diketones, are compounds have a variety of applications on synthesis, coordination chemistry, and biochemistry. Acetylacetone (AA) is the simplest form of β-diketones, tautomerizing between enol form and keto form with an equilibrium constant depending on solvents. In this work, the enol-keto tautomerization of acetylacetone (AA) in water, methanol, ethanol, acetonitrile, and their deuterated solvents was investigated using ultraviolet (UV) spectroscopy and nuclear magnetic resonance (NMR). The results reveal that AA tautomerization follows first order kinetics when isotope exchange is not involved. The tautomerization rates of AA in solvents are water > alcohols > acetonitrile. In addition, base catalytic effects in CH_3CN and alcohols are determined to be 269 and 1715 s^{-1} M^{-1}, respectively. Acid catalytic effects are insignificant in all studied solvents except in CH_3CN, where a weak catalytic effect of 4.19 s^{-1} M^{-1} is observed. Water catalytic effects are 1.69×10^{-4} and 1.51×10^{-3} s^{-1} M^{-1} in CH_3CN and alcohols, respectively. To account for the non-exponential behavior due to the isotope exchange, two kinetic models were proposed to simulate the concentration profiles under both base-free and base-catalyzed conditions. The results suggest that AA tautomerization and isotope exchange proceed concurrently, facilitated by the solvent bridge and the enolate intermediate. Moreover, the enolate form enables isotope exchange in the absence of tautomerization. Finally, kinetic isotope effects (KIEs, k_H/k_D) of AA tautomerization in water and methanol are determined to be 6.15 ± 0.39 and 6.35 ± 0.17, respectively.

Keywords: acetylacetone, tautomerization, reaction kinetics, UV absorption spectroscopy, NMR, kinetic isotope effect.

doi:10.6342/NTU202503041

CONTENTS

doi:10.6342/NTU202503041

doi:10.6342/NTU202503041

LIST OF FIGURES

doi:10.6342/NTU202503041

doi:10.6342/NTU202503041

doi:10.6342/NTU202503041

LIST OF TABLES

doi:10.6342/NTU202503041

Chapter 1 Introduction

1.1 Acetylacetone (AA) tautomerization

β-diketones, also known as 1,3-diketones, are compounds have a variety of applications on synthesis, industry, coordination chemistry, and biochemistry. For instance, curcumin has been seen as one of promising compounds for the treatment of Alzheimer's disease.[1] Dibenzoylmethane and its derivatives are widely used in sunscreen products owing to their ultraviolet (UV) filter property.[2] In addition, β-diketones also bind to transition metals and lanthanide ions with two oxygen atoms to form complexes, affecting reactions including enol-keto tautomerization.[3-6]

Acetylacetone (AA) is the simplest form of β-diketones, tautomerizing between keto and enol form with an equilibrium constant depending on solvent as shown in Figure 1. It is not only a fundamental unit used in synthesis for its simplicity[6, 7] but also a chelating ligand used to bind metals effectively.[6] In addition, the acid dissociation constant (K_a) of AA is ca. $10^{-8.9}$,[8-10] indicating a weak acid in water.

The enol-keto tautomerization is an important concept in chemistry which has been studied over a century, affecting reactions with various applications.[2] As the simplest form of β-diketones, AA is often used as an example for studying the tautomerization. Typically, UV spectroscopy,[9, 11-15] infrared (IR) spectroscopy,[16, 17] and nuclear magnetic resonance[12, 14, 18-23] (NMR) are used for studying equilibrium and kinetics of the tautomerization. As shown in Figure 1, the enol form of AA has a $\pi \rightarrow \pi^*$ transistion which is enhanced by the conjugated structure, resulting in a stronger absorption coefficient than that of the keto form.[11-13] Since the keto form of AA is hard to measure directly with UV method, NMR is usually used to decide the equilibrium constant of the tautomerization. The equilibrium of neat AA favors enol form due to the intramolecular

doi:10.6342/NTU202503041

hydrogen bonding, and the enol fraction is ca. 80% reported by several works.[16, 21]

To the best of our knowledge, there has been a lot of studies focused on the thermodynamics of AA tautomerization in solvents, discussing how the polarity of solvent relates to the equilibrium constant of tautomerization.[12, 13, 23] The comparison of AA equilibrium constants and solvent dielectric constants reported in the literatures[22-25] and this work is summarized in Table 1. In general, AA exhibits higher equilibrium constants in solvents with lower polarity. In addition, the kinetic effects of AA tautomerization including base addition[9, 13-15], water content[12, 26], and metal addition[4, 13] are also found. However, few studies have addressed the kinetics of tautomerization involving the isotope exchange,[22] discussing the model of tautomerization if base and isotope were involved. Though Nichols *et al.* studied AA tautomerization in d4-methanol and proposed a model describing the relationship between the tautomerization and the isotope exchange,[22] their model is over-simplified. The mechanism of AA tautomerization including base and isotope exchange remains obscure.

In this work, we use UV spectroscopy and NMR to detect AA tautomerization in water, methanol, ethanol, acetonitrile, and their deuterated solvents. Besides that, we not only add sodium hydroxide (NaOH) and triethylamine (TEA) to verify base catalyzation but also add hydrogen chloride (HCL) and sulfuric acid (H_2SO_4) to identify the acid catalytic effect. As a result, we verify equilibrium constants and kinetics of AA tautomerization in normal solvents and propose two mechanisms to explain the tautomerization involving isotope exchange and the base catalytic effect. This study not only demonstrates that AA tautomerization without isotope exchange follows first-order kinetics catalyzed by water and base, but also explains the observed non-exponential behavior using the proposed models.

doi:10.6342/NTU202503041

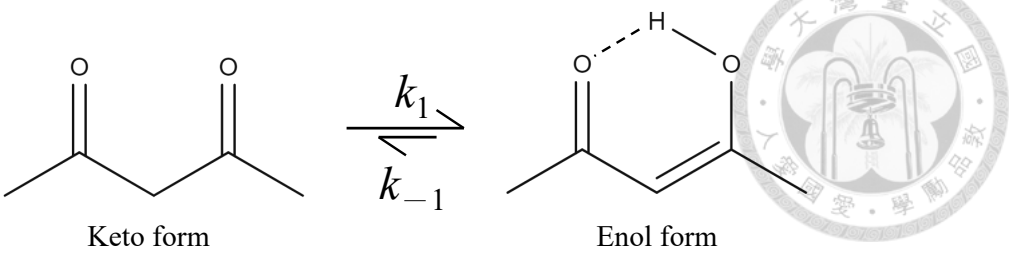

Figure 1 Keto-Enol tautomerization of acetylacetone (AA)

Note that the enol form has intramolecular hydrogen bonding which makes the equilibrium favoring enol form in organic solvents. The enol form of AA has a $\pi \rightarrow \pi^*$ transition which is enhanced by the conjugated structure, resulting in a stronger absorption coefficient than that of the keto form (see **section 3.1**).

Table 1 Comparison of AA equilibrium constants in solvents and solvent dielectric constants reported in literatures and this work

AA in solvents	K_{eq} this work	K_{eq} literatures	Enol fraction[e] literatures	Dielectric constants @ 20°C
Neat		4.81[a]	0.83	25.7[c]
Water	0.18	0.23[b]	0.19	80.4[c]
Acetonitrile (MeCN)	1.3	1.2[b]	0.55	37.5[c]
Methanol (MeOH)	2.6	2.9[b]	0.74	33.6[c]
Ethanol (EtOH)		5.8[b]	0.85	25.2[d]

a Nichols *et al.* work[22]

b Mills *et al.* work[23]

c Maryott *et al.* work[24]

d Gregory *et al.* work[25]

e Calculated from [Enol] / ([Enol]+[Keto])

doi:10.6342/NTU202503041

Chapter 2 Experimental section

2.1 Materials

Normal solvents: Acetylacetone (AA, Sigma-Aldrich, 99.1%), methanol (HoneyWell, > 99%), ethanol (HoneyWell, > 99.8%), acetonitrile (HoneyWell, > 99%), and deionized (DI) water (18.2 MΩ×cm).

To identify isotope effect, we used deuterated solvents including d4-methanol (thermo-scientific, atom-D > 99.8%), d3-acetonitrile (thermo-scientific, atom-D > 99%), and deuterium water (D_2O, Sigma-Aldrich, atom-D > 99.9%). All studied solvents were used as purchased without further purification.

2.2 pH measurement

In order to identify the catalytic effects of acid and base. Sodium hydroxide (NaOH, Showa Chemicals), used as a catalyst, was dissolved in DI water and then titrated with potassium hydrogen phthalate (KHP, Scharlau, > 99.9%). Finally, hydrogen chloride (HCL, Fisher) diluted in DI water solution was titrated using the titrated NaOH solution.

2.2.1 pH meter

Since AA tautomerization in organic solvents is catalyzed by base,[9, 14, 15] the pH meter (Horiba, F-51) equipped with the electrode (LAQUA, 9681S-10D) was used to verify residual base in the organic solvents. The pH meter was calibrated using standard solution of buffer (Rocker, pH = 4.01, 7.00, 10.01) prior to measurements. The error between measured pH value and titrated concentration of sodium hydroxide solution was ca. 7%. Although the measured concentration of proton was proportional to the titrated solution in water, the electrode didn't perform as reliably in methanol as it did in water.

doi:10.6342/NTU202503041

Nevertheless, the measurement of residual base using titration combined with pH meter remained feasible.

2.3 Kinetics measurement

AA tautomerization was measured by UV absorption spectroscopy and NMR, and the procedure was described below.

2.3.1 UV absorption spectroscopy

The experiments were conducted using a D_2 lamp (Hamamatsu, L10904) as the light source and a spectrometer (Ocean optics, Flame-S-XR1-ES) as the detector. To ensure proper mixing, the solution was stirred at 1200 rpm using a stir bar controlled by a magnetic stirrer. The cuvette (10×10×45 mm), secured with a homemade 3D-printed device, was positioned such that the aligned light path passed through its center. The temperature was only controlled by the air conditioner and measured by a calibrated thermometer (Rotronic, HC2A-S). The picture of device is shown in Figure S1.

AA was introduced by one of following two methods: either by diluting it in one solvent (solvent 1, already in pre-equilibrium) and adding it to another solvent (solvent 2) with a micropipette, or by injecting vapor using a syringe. For example, a 20 μL portion of the AA solution or 0.4 mL of saturated AA vapor (T=23–25°C) was added to 2 mL of another solvent. As the result, AA concentration was typically around 5×10^{-5} M, corresponding to an absorbance range of 0.1 to 1.0 at 272 nm, the maximum absorption wavelength of AA. Finally, the data were collected by LabVIEW and processed by a homemade MATLAB code.

2.3.2 80 MHz NMR

2.3.2.1 Data acquisition

For the convenience of obtaining the spectrum quickly after adding AA, 80 MHz

doi:10.6342/NTU202503041

benchtop NMR (Bruker, F80) was used. The probe is an internal probe (PHF-DUL80B-H/C/F-5.0-Z). The pulse sequence diagram is shown in Figure 2. Briefly, spectra were acquired with a 2.54 s acquisition time using a 90° excitation pulse with an excitation time (P1) of 10.9 μs. The recycle delay time (D1) was set to exceed five times the longest relaxation time (T1) of the AA peaks. For instance, the longest T1 of AA in d3-acetonitrile was measured as 4.8 s, so D1 was set to 25 s. The number of scans (ns) was adjusted based on the reaction time in different solvents, typically set to 1, 10, 20, or more. As a result, the latency including mixing time was approximately 70 s. In most cases, 10 μL of neat AA liquid was introduced into 0.6 mL of solvent using a syringe, resulting in an AA concentration of 0.16 M, which provided a sufficiently good signal-to-noise ratio (S/N ratio). Finally, the pseudo 2D (intensity vs. chemical shift and time) proton (^{1}H) spectra were performed at z-axis pulsed field gradient with a series of ns at 25.0°C.

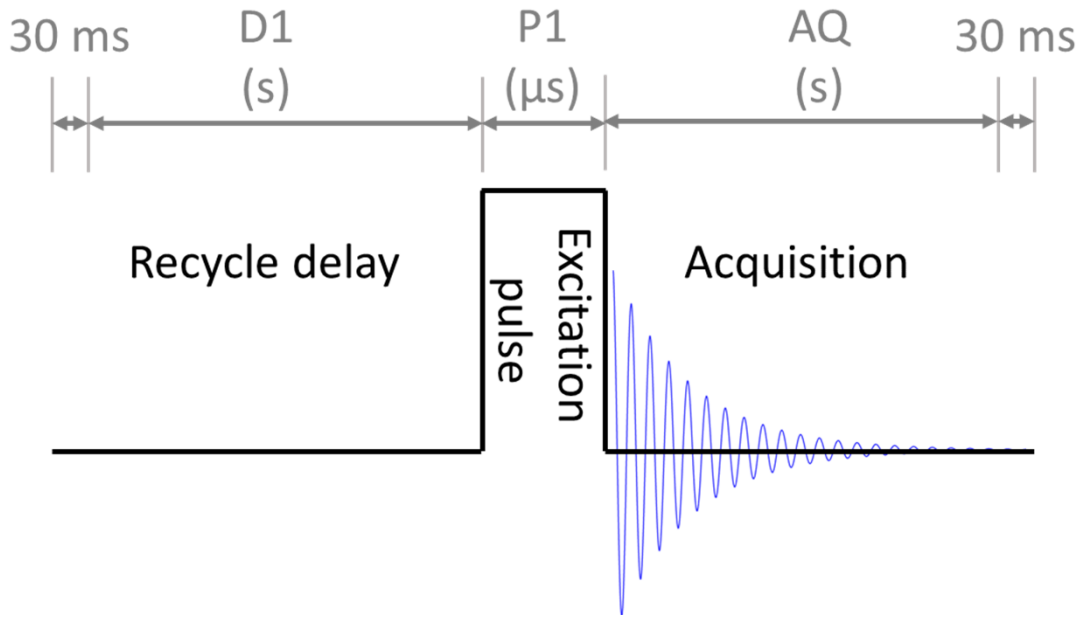

Figure 2 Diagram of NMR pulse sequence.

Where D1 is the recycle time for the delay; P1 is the excitation time of the pulse; AQ is the time for acquisition of free induction decay (FID) signal.

doi:10.6342/NTU202503041

2.3.2.2 Data processing

Spectra were processed using Topspin software (version 4.3.0), and the phase was corrected manually. Though we neither used the capillary tube with an inner tube to add an internal standard nor added the internal standard (TMS or DSS) for all of the kinetic measurements, assignments of AA peaks were identified by the solvent peak of the initial DSS contained solution and used for the remaining experiments. For a clearer identification, AA peaks are named and listed in Table 2 as an example. Since the chemical shifts in various solvents have been well-studied, the chemical shifts of spectra done by 80 MHZ NMR are referenced to the enol 6H at 2.044 ppm for easier comparison.

Table 2 AA peaks' assignments in D_2O (see Figure S2) and names in this work

AA in D_2O	Enol-CH_3	Keto-CH_3	Keto-CHD	Keto-CH_2	Enol-CH
Name	Enol 6H	Keto 6H	Keto HD	Keto 2H	Enol 1H
Chemical shift[a] / ppm	2.10	2.30	3.83, 3.86, 3.89	3.88	5.75
Peak splitting	singlet	singlet	triplet	singlet	singlet

a. Peaks are referenced to HOD solvent peak, 4.80 ppm in D_2O.

To process the overlapping peaks caused by the low magnetic field, we used matNMR[27] (version 3.9.0, a MATLAB-based code developed by Jacco D. van Beek) to extract the data points of the spectra. Then, a homemade code was used to fit and integrate the peaks. If the baseline was lower than 10% of the signal maximum, it was fitted linearly. Otherwise, the baseline was subtracted using other fitted peaks. Finally, peaks were fitted using a Lorentzian equation (E1)

$$L(x) = \frac{Hw^2}{w^2 + (x - x_0)^2} \qquad \text{(E1)}$$

doi:10.6342/NTU202503041

where H is the peak height, w is one-half of the full width at half maximum (FWHM), x is the chemical shift in the unit of ppm, and x_0 is the peak center in the unit of ppm. The reason that the spectral line shape of peak in NMR is typically Lorentzian in the frequency domain is the exponential function of FID in the time domain.[28] In cases of overlapping peaks, a multi-function fitting approach (multi-E1) was applied. Finally, the fitted peaks were integrated over the range from 0 to 16.5 ppm.

2.3.3 600 MHz NMR

2.3.3.1 Data acquisition and processing

^{1}H spectra were recorded at a temperature of 25.0°C using a high magnetic field NMR (Bruker, AVIII 600; probe: CPTCI 1H-13C-15N/D Z-GRD) to study the base catalytic effect in CD_3CN. The pulse sequence diagram is shown in Figure 2. T1 of AA peaks in CD_3CN were measured and summarized in Table 3. Briefly, spectra were acquired with a 1.24 s acquisition time using a 30° excitation pulse with an excitation time (P1) of 2.16 μs. Since the longest T1, observed in keto HD was ca. 8.8 s, D1 was set to 30 s to ensure full relaxation. The number scan was set to a multiple of 8 to cancel out the error during averaging. The spectra were manually phased, and chemical shift was corrected by signal reference (S_R) which had been referenced to TMS. Finally, peaks were integrated between the chemical shifts corresponding to one percent of the peak's maxima intensity, except the overlapping peaks which were integrated to the chemical shift of the intensity valley.

Table 3 T1 measurement of AA in CD_3CN conducted in the 600 MHZ NMR

AA in CD_3CN	Enol 6H	Keto 6H	Keto HD	Keto 2H	Enol 1H
T1 / s	4.78	6.21	8.80	6.31	7.76

doi:10.6342/NTU202503041

2.3.4 Monte-Carlo method and tautomerization mechanisms

Monte-Carlo method has been a well-known method for solving problems using random numbers for decades.[29, 30] Here, it was used to acquire the rate constants by simulating time profiles with proposed mechanism 1 and 2 as shown in Figure 3 and Figure 4, respectively. Detailed discussions of the mechanisms are provided in the **section 3.3 to 3.6**.

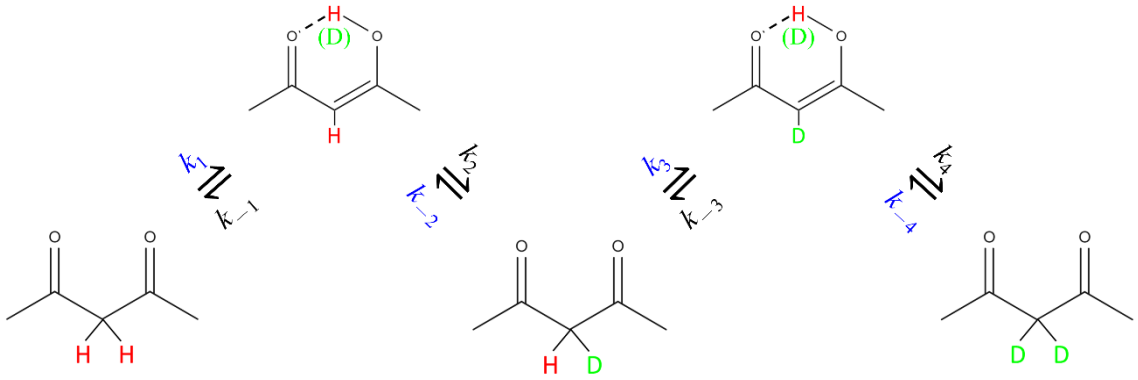

Figure 3 Proposed mechanism 1 of AA tautomerization without base catalysis.

Where k_1 — k_4 are the forward rate constants, and k_{-1} — k_{-4} are the reverse rate constants.

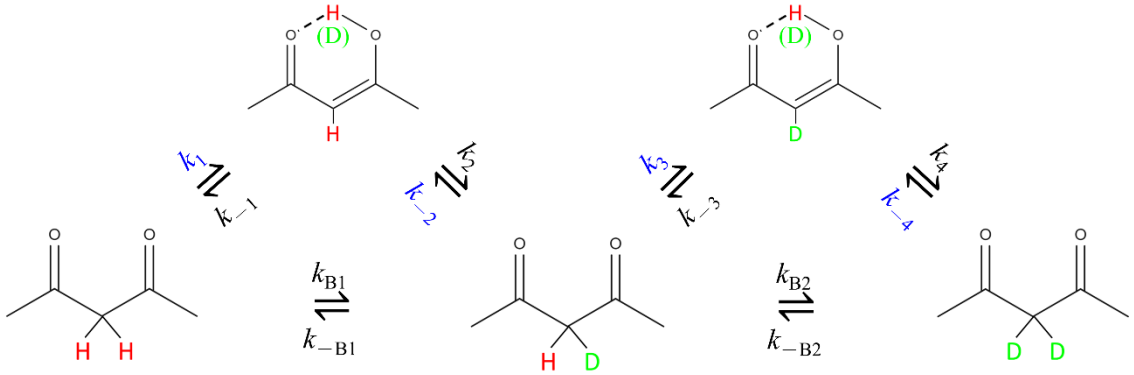

Figure 4 Proposed mechanism 2 of AA tautomerization with base catalysis.

Where k_1 — k_4, k_{B1}, k_{B2} are the forward rate constants, and k_{-1} — k_{-4}, k_{-B1}, k_{-B2} are the reverse rate constants. Comparing to the mechanism 1, other paths assisted by base (see **section 3.3.2**) are assumed to exchange hydrogen isotopes between keto forms.

doi:10.6342/NTU202503041

The simulating curves were obtained by the rate equations and boundary conditions presented in Figure S3 and Figure S4 for mechanism 1 and 2, respectively. Here, the boundary conditions include the equilibrium constants, and total concentrations of the enol and keto forms. Reverse rate constants were determined from the forward rate constants due to the fixed equilibrium constants. Global fits were performed by varying variables such as the forward rate constants and the initial keto fraction of AA.

The time intervals of the curves were set at least 700 times shorter than the shortest fitting lifetime. The error was presented as 0.5 — 1 standard deviation which was obtained by the least square of signal (E2) and the definition of standard deviation (E3)

$$S_R^2 = \sum (\text{Signal of Simulation} - \text{Signal of Experiment})^2 \qquad \text{(E2)}$$

$$\sigma = \sqrt{\frac{S_R^2}{n-1}} \qquad \text{(E3)}$$

where S_R^2 is the residual square of signals; n is the number of data points in the experiment; σ is the standard deviation. To further investigate the relationships between variables and assess their reliability, fits of variable pairs were performed with the remaining variables fixed at values obtained from the global fitting.

doi:10.6342/NTU202503041

Chapter 3 Results and Discussion

3.1 AA UV absorption

3.1.1 Solvatochromic effect

To effectively apply Beer-Lambert law, we select the maximum absorption wavelength (λ_{max}) for analysis of the kinetic measurements. As shown in Figure 5, λ_{max} of AA is ca. 272 ± 1 nm in solvents including water, acetonitrile, methanol, ethanol, and isopropanol (IPA). Watarai *et al.* reported a similar λ_{max} at 271 nm[15] which affects little to kinetic analysis this work. This phenomenon, where solvents interact with AA, influencing the energy gap of the $\pi \rightarrow \pi^*$ transition[11, 13] and thereby affecting the λ_{max} of AA enol form, is referred to the solvatochromic effect. Although the λ_{max} of AA does not exhibit a clear trend with the polarity of solvents, the solvatochromic effect is weak. Consequently, 272 nm was chosen for the kinetic analysis of AA tautomerization in every solvent.

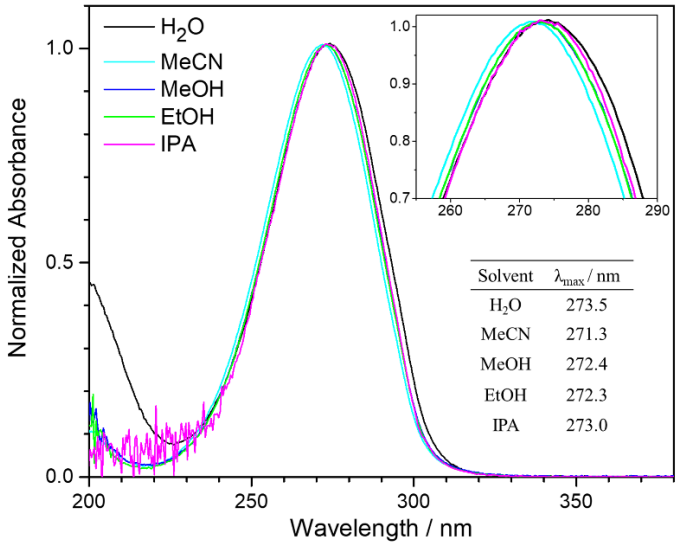

Figure 5 Normalized absorption spectra of AA in various solvents.

(H_2O = water, MeCN = acetonitrile, MeOH = methanol, EtOH = ethanol, and IPA = isopropanol). The data indicate that the solvatochromic effect of AA is weak, with the

doi:10.6342/NTU202503041

maximum absorption wavelength λ_{max} being at 272 ± 1 nm (272 nm was chosen for analyzing the kinetics in the UV experiments).

3.1.2 Molar absorption coefficient

With the enol fraction calculated from concentration ratio of enol form (E4) obtained by ^{1}H spectra, we further investigated the molar absorption coefficient of AA at 272 nm in solvents. The molar absorption coefficient was obtained by the observed absorbance (1 cm cuvette) and the AA concentration in normal solvents.

$$\text{Enol fraction, } f = \text{Integration area of } \frac{\text{Enol 6H}}{\text{Enol 6H} + \text{Keto 6H}} \qquad \text{(E4)}$$

As shown in Figure 6, the apparent molar absorption coefficient (ε) fits linearly against enol fraction, and the fitting equation is $\varepsilon = (10742 \pm 789)f + (25 \pm 348)$ with one standard deviation (SD). As the result, ε of enol and keto form of AA at 272 nm are 10742, and 25 M^{-1} cm^{-1}, respectively. Watarai *et al.* did the AA tautomerization in the binary aqueous mixtures of dioxane, methanol, and ethanol and gave the similar results, with ε of enol and keto form of AA at 273 nm are 10760 ± 60, and 249 ± 28 M^{-1} cm^{-1}, respectively.[12] Since the absorption of the keto form is at least less than 2%, the contribution of the keto form to absorbance is ignored. Messaadia *et al.* investigated the cross sections of 2,3-pentanedione and 2,4-pentanedione (AA) in gas phase,[11] and they stated that the weak absorption of the keto form of AA is due to the n → π* forbidden electronic transition. In contrast, the high absorption coefficient of the enol form of AA is attributed to the π → π* allowed electronic transition and the chromophores formed by the conjugated π-bond system.

doi:10.6342/NTU202503041

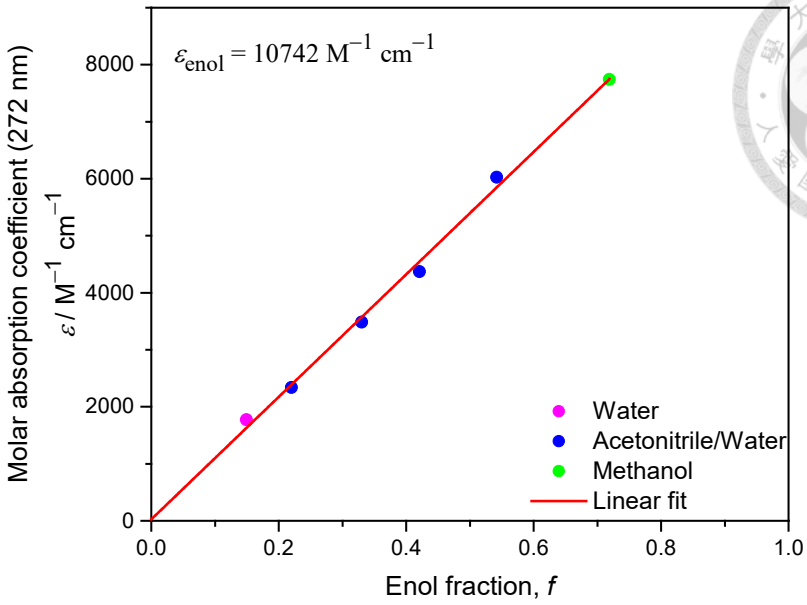

Figure 6 The apparent molar absorption coefficient ε at 272 nm of AA against the enol fraction f in solvents.

The apparent molar absorption coefficient was deduced from the observed absorbance (1 cm cuvette) and the concentration of AA in normal solvents. The enol fraction was calculated from the equilibrium concentrations in deuterated solvents in NMR experiments. Here, we assume that the solvent isotope effect in enol fraction is weak. Minor effect of solvent 1 was not corrected due to its low percentage (1–3% v/v). Linear fit to the data points gives $\varepsilon = (10742 \pm 789)\, f + (25 \pm 348)$; the error bars indicate one standard deviation (SD). As the result, the data indicate that the molar absorption coefficient of the enol form is 1.07×10^4 M^{-1} cm^{-1}, and the absorption of the keto form is negligible.

3.2 First-order kinetics

To study the different directions of AA tautomerization, AA was first diluted in solvent 1. After waiting for more than 50 times the lifetime of tautomerization to ensure equilibrium, it was added to solvent 2, and changes between the equilibrium of two

doi:10.6342/NTU202503041

solvents were recorded. Time profiles of AA dilutions from water to methanol and acetonitrile are shown in Figure 7, demonstrating good fits with the first-order kinetics described by (E5)

$$A(t) = A_{\mathrm{eq}} + \left(A_0 - A_{\mathrm{eq}}\right)\exp(-t/\tau) \qquad \text{(E5)}$$

when $t/\tau << 1$,

$$A(t) = A_0 + \left(A_{\mathrm{eq}} - A_0\right)k_{\mathrm{obs}}t \qquad \text{(E6)}$$

where A_0 is the extrapolated absorbance of the enol form at the starting of the reaction (the moment of adding AA, $t = 0$); A_{eq} is the absorbance of the enol form at equilibrium; τ is the lifetime which is the reciprocal of the observed reaction rate constant, $\tau = k_{\mathrm{obs}}^{-1}$. As a result, τ of AA tautomerization in methanol and acetonitrile are 102 s and 2132 s, respectively. In fact, the first-order kinetics of AA tautomerization has been described by several works.[4, 9, 12-16, 22, 26] Watarai *et al.* conducted experiments on the AA tautomerization in various solvents, including water, methanol, ethanol, acetonitrile, dioxane, and dimethyl sulfoxide (DMSO).[12] They also observed that the tautomerization rate was much slower in acetonitrile than that in methanol. These results reveal that the exchangeable hydrogen in the solvent helps the tautomerization, and it follows first-order kinetics.

doi:10.6342/NTU202503041

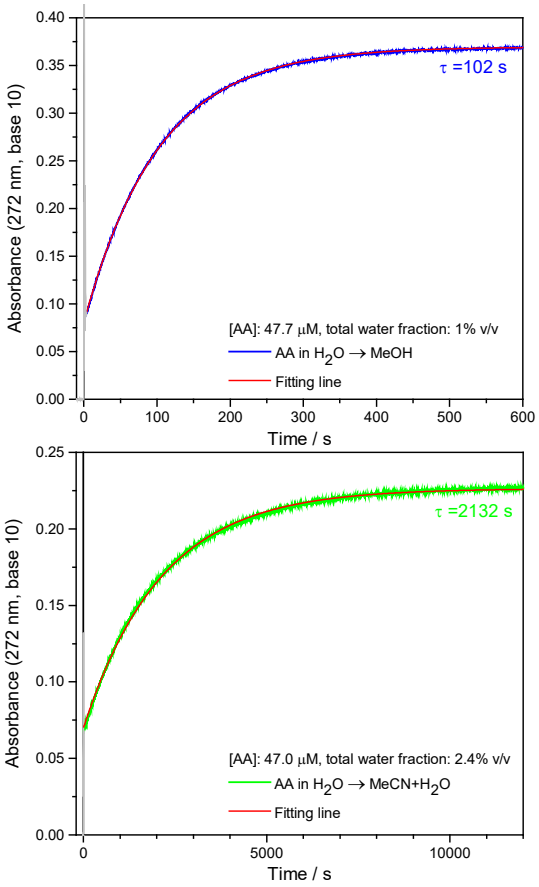

Figure 7 Observed time profiles of AA tautomerization from water to methanol (upper panel) and acetonitrile (lower panel).

The gray lines indicate the solutions were still mixing ca. 4 s, and the red lines are first-order fits of (E5). The lifetimes in methanol and acetonitrile are 102 and 2132 s, respectively.

3.3 Acid-base catalytic effect

We also investigated the catalytic effects of acid and base on the AA tautomerization in alcohols, acetonitrile, and water by adding $HCL_{(aq)}$ and $H_2SO_{4(aq)}$ as acids; $NaOH_{(aq)}$ and triethylamine (TEA) as bases.

doi:10.6342/NTU202503041

3.3.1 Catalytic effects of NaOH and HCL in solvents

As shown in Figure 8, NaOH catalysis is significant for AA tautomerization in alcohols and acetonitrile with slopes of 1715 ± 195 and 269 ± 106 s^{-1} M^{-1} (± 1 SD), but it is insignificant for water. Acid catalysis is not observed for AA tautomerization in water and alcohols, however it is weak for acetonitrile with a slope of 4.19 ± 0.47 s^{-1} M^{-1} (± 1 SD).

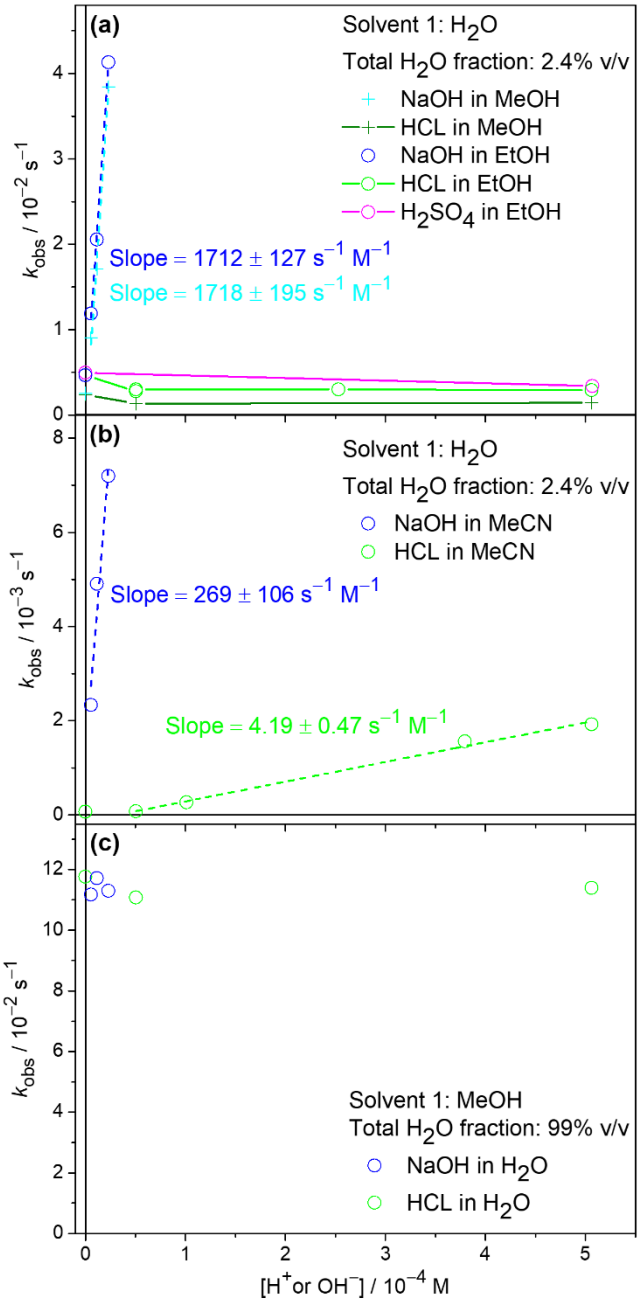

doi:10.6342/NTU202503041

Figure 8 The catalytic effects of acid and base to the tautomerization rate coefficients of AA in (a) alcohols, (b) acetonitrile, and (c) water.

Experimental conditions: [AA] = 5×10^{-5} M; T = 23.1°C. Here, we chose NaOH as base; HCL or H_2SO_4 as acid. The dashed lines are linear fits. Base catalysis is significant for alcohols and acetonitrile solvents with slopes of ca. 1715 and 270 s^{-1} M^{-1}, respectively, except for water. Acid catalysis is not observed for water and alcohols solvents, but it is observed to have a weak effect for acetonitrile with a slope of 4.19 s^{-1} M^{-1}. Note that unacidified solvents might contain some residual base (see Figure 12).

The equations of linear fits of base and acid catalytic effects are described by (E7) and (E8), respectively.

$$k_{\mathrm{obs}} = k_0 + k_{\mathrm{B}}[\mathrm{Base}] \quad \text{(E7)}$$

$$k_{\mathrm{obs}} = k_0 + k_{\mathrm{A}}[\mathrm{Acid}] \quad \text{(E8)}$$

where k_0 is the extrapolated rate of solvent without base and acid in the unit of s^{-1}; k_B and k_A are the catalytic coefficients of base and acid, respectively, with units of s^{-1} M^{-1}. Several works also mentioned the catalytic effect of base on the AA tautomerization though different bases were used.[9, 13-15] For example, Watarai *et al.* measured the catalytic effects of acetate and monochloro acetate anion in water and reported that k_B of those were 19.7 and 2.2 s^{-1} M^{-1}, respectively.[14] Bruice measured the catalytic effect of amines in water by a stopped-flow spectrophotometer equipped with a waveform recorder, which offered a better time resolution than that in our work (0.2 s^{-1}) and allowed for higher [amines] than [NaOH] used in our work due to the higher pK_a of NaOH. These results support the existence of base catalysis even in water.[9]

doi:10.6342/NTU202503041

3.3.2 Proton abstraction mechanism

Comparing to the base catalytic effect, the acid catalytic effect for AA tautomerization is weak in acetonitrile and becomes insignificant in water and alcohols. The weak catalytic effect of Lowry-Brønsted acid has been mentioned in a few works.[13] It demonstrates that acid catalysis undergoes a different mechanism compared with that of base catalysis which catalyzes the tautomerization by abstracting protons.[9] The mechanism is shown in Figure 9, the acidic hydrogen in AA keto form[8-10] is attacked by base, forming the enolate intermediate and catalyzing the tautomerization.

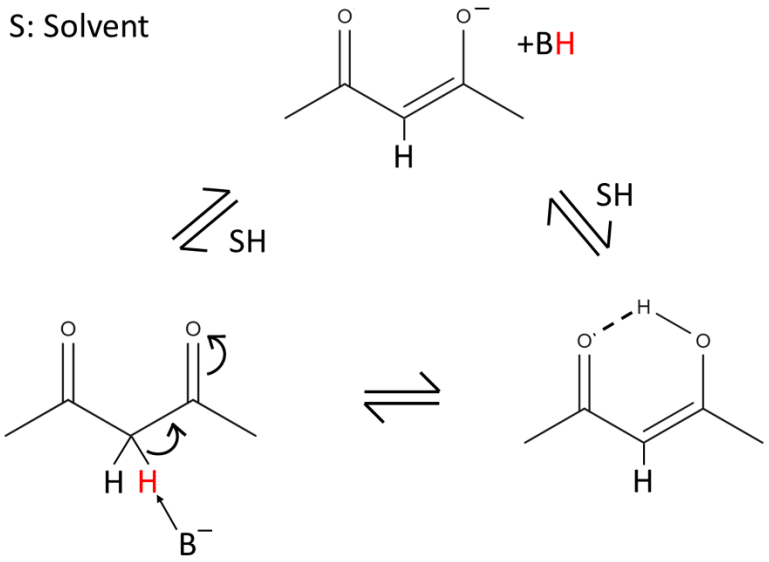

Figure 9 Mechanism of proton abstraction of base in AA tautomerization.

Here, SH is the solvent molecule that contains a transferable hydrogen atom.

3.3.3 Catalytic effect of TEA in acetonitrile

In order to verify the base effect, TEA was chosen as the other base. As shown in Figure 10, AA tautomerization is also catalyzed by TEA with slopes of 630 ± 15–759 ± 32 s^{-1} M^{-1} (± 1 SD), corresponding to 0–2.26 M water concentrations, respectively. Data are summarized in Table S1. Watarai *et al.* also measured the catalytic effect of

doi:10.6342/NTU202503041

triethylamine (TEA) and tributylamine (TBA) in solvents and reported that k_B of those in acetonitrile were 588 and 202 s^{-1} M^{-1}, respectively.[15] The k_B of TEA shows ca. 7% error at 0 M water concentration which is acceptable considering the low concentration (10^{-5}–10^{-4} M).

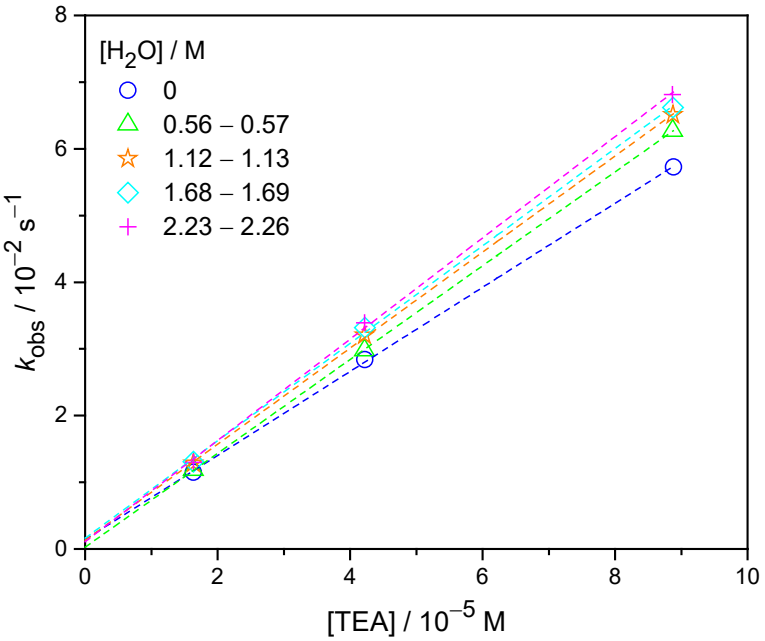

Figure 10 The catalytic effect of TEA to the tautomerization rate coefficients of AA with different water concentrations in acetonitrile.

Experimental conditions: [AA] = 6.6×10^{-5} M; T = 25.1 ± 0.1°C. Data are summarized in Table S1. The dashed lines are linear fits described by (E7). Base catalysis is significant for AA tautomerization in acetonitrile with slopes of 630 ± 15–759 ± 32 s^{-1} M^{-1} (± 1 SD), corresponding to 0–2.26 M water concentrations, respectively.

3.3.3.1 Synergistic catalysis of TEA and water

Water also catalyzes the tautomerization shown in Figure 11 though the effect is weaker than that of base. Note that the tautomerization is catalyzed not only by base and water individually but also by both of them synergistically. The equation is described by (E9)

doi:10.6342/NTU202503041

$$k_{obs} = k_0 + k_B[\text{Base}] + k_W[H_2O]^m + k_{BW}[\text{Base}][H_2O]^n \quad \text{(E9)}$$

where k_0 is the extrapolated rate of AA tautomerization in solvent without base and water in the unit of s^{-1}; m and n are reaction orders of water molar concentration for water catalysis and synergistic catalysis of base and water, respectively. k_W is the catalytic coefficient of water in the unit of s^{-1} M^{-m}; k_{BW} is the coefficient of synergistic catalysis of base and water in the unit of s^{-1} $M^{-(n+1)}$. Besides, the non-first-order dependence on water concentration shown in Figure 11 indicates water catalyzes the reaction through a multi-step mechanism rather than simple elastic collisions.

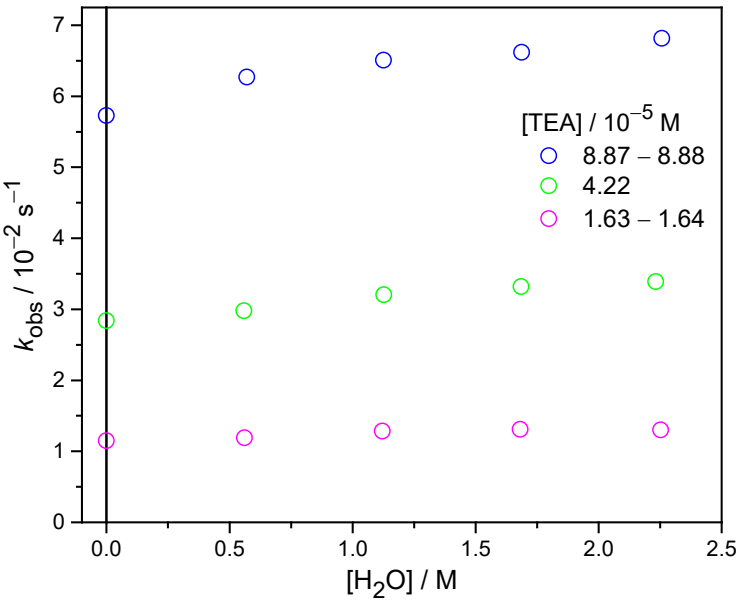

Figure 11 The effect of water to the tautomerization rate coefficients of AA with different TEA concentrations in acetonitrile.

Experimental conditions: [AA] = 6.6×10^{-5} M; T = 25.1 ± 0.1°C. Water catalysis is weak for AA tautomerization in acetonitrile. Same data as Figure 10.

3.4 Residual base in solvents and cuvettes

Note that commercial solvents of alcohols and acetonitrile may contain "residual base". As shown in Figure 12, we estimated the residual base in acetonitrile by the

doi:10.6342/NTU202503041

observed tautomerization rate and k_B of NaOH and found that $[OH^-] =\sim 1.7$ μM firstly (blue line). Secondly, HCL was added to neutralize the residual base in the controlled experiment, giving an extremely slow tautomerization rate. By fitting it linearly, the slope was $(3.62 \pm 4.92)\times10^{-8}$ s^{-1} with one standard error. The observed rate constant, k_{obs} was estimated by (E6), giving as $(2.25 \pm 3.02)\times10^{-7}$ s^{-1} (lifetime > 500 hours!). Finally, the AA equilibrium in acetonitrile in the controlled experiment was verified by the following NaOH addition. The result implies that acetonitrile catalyzes AA tautomerization weakly. Comparing to the catalytic effects of water and alcohols, we suggest that the tautomerization is catalyzed by solvents' transferable protons, in other words, intermolecular proton transfer.

Also, the extremely slow rate of the tautomerization in the neutralized acetonitrile implies the intramolecular proton transfer of AA is weak, and the observed tautomerization rate is mainly from the catalytic effect of intermolecular proton transfer assisted by the residual base or water. In conclusion, the strong catalytic effect of base highlights that the need for careful consideration of potential base from the solvent or the cuvette when quantifying tautomerization rates.

doi:10.6342/NTU202503041

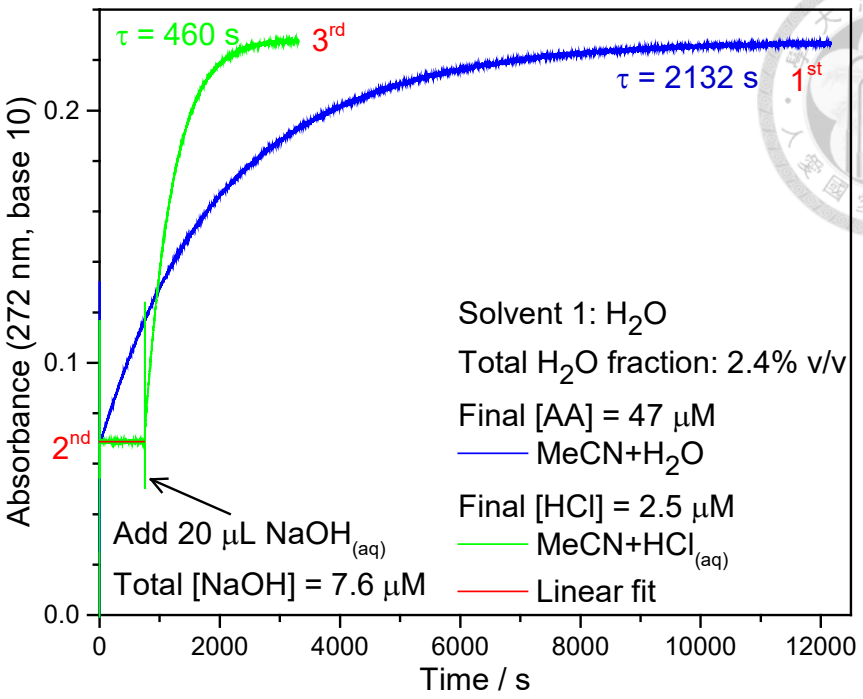

Figure 12 Time profiles of absorbance change of AA tautomerization in acetonitrile. Experimental conditions: [AA] = 47 μM; T = 23.3°C. 1st run (blue trace): AA diluted in water was added to acetonitrile and the lifetime of 2123 s was observed. 2nd run (green trace before 750 s): a repeated experiment with conditions are the same as the 1st run, except 2.5 μM of HCL was additionally spiked to neutralize the residue base in the solvent. The tautomerization reaction became much slower, with a slope of $(3.62 \pm 4.92)\times10^{-8}$ s^{-1}, suggesting $k_{obs} = (2.25 \pm 3.02)\times10^{-7}$ s^{-1}. 3rd run (green trace after 750 s): 7.6 μM of NaOH was further added to the end solution of the 2nd run to catalyze the tautomerization. A lifetime of 460 s was observed. The total water fraction was 2.4% v/v for the 1st and 2nd runs, 3.4% v/v for the 3rd run.

doi:10.6342/NTU202503041

3.5 Water catalytic effect

3.5.1 Rates in binary solvents (water and organic solvent)

To investigate the influence of water on the tautomerization rates in different organic solvents, AA was added to solvent 2 with varying organic mole fractions (X_s). Data are summarized in Table S2. As shown in Figure 13, the concentration of 3.39×10^{-4} M for HCL was added to alcohols to neutralize the residual base, but it was not added to acetonitrile due to its acid catalytic effect (Figure 8(b)). Consequently, the tautomerization rates in solvents decreases in the following order: water > alcohols > acetonitrile. The water catalytic effect in methanol is similar to that in ethanol, but it is weaker than that in acetonitrile. Note that water has a stronger catalytic effect on the tautomerization rates in alcohols at lower water mole fractions (high X_s), indicating that the water catalysis is more pronounced below a specific amount of water.

doi:10.6342/NTU202503041

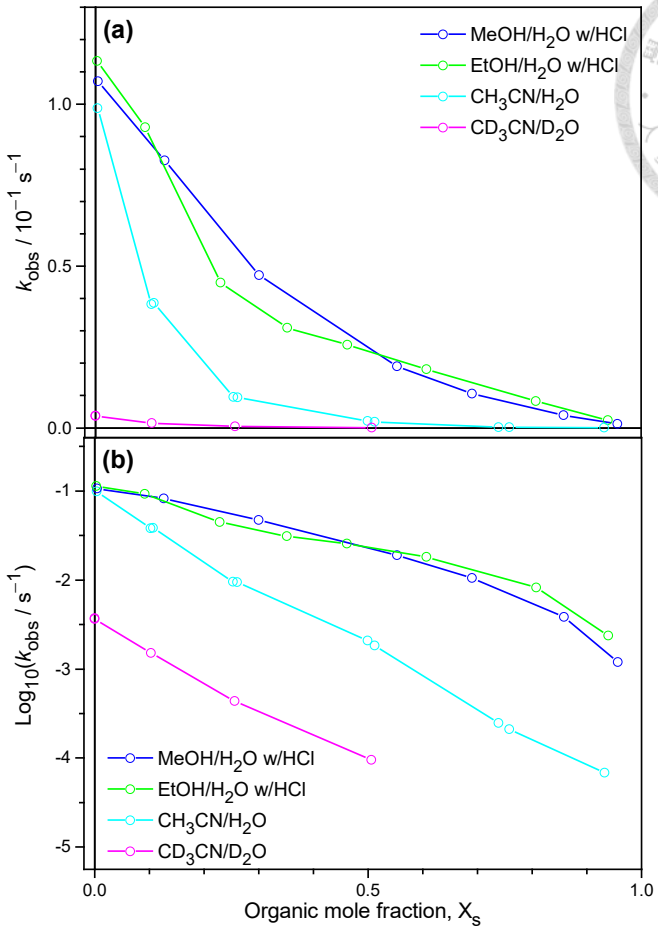

Figure 13 Effects of organic solvents mixed with water in the tautomerization reaction kinetics of AA.

Experimental conditions: [AA] = 4.86×10^{-5} M; T = 23.2°C. Data are summarized in Table S2. (a) The observed rate coefficient (k_{obs}) against mole fraction of organic solvents (X_s); (b) The same data but with k_{obs} plotted in logarithm scale. Solvent 1 was water or alcohols for alcohols/H_2O; water or CH_3CN for CH_3CN/H_2O; neat AA liquid for CD_3CN/D_2O. We added HCL (3.39×10^{-4} M) to neutralize possible residue base in alcohols solvents. However, it was not added to acetonitrile due to its catalytic effect shown in Figure 8(b). Note that the tautomerization rates in CD_3CN/D_2O were obtained in NMR experiments, and the change of enol 6H were fitted with first-order kinetics (E5), though a detailed mechanism for tautomerization involved isotope exchange is proposed (see Figure 3).

doi:10.6342/NTU202503041

In addition, the results are compared to Watarai *et al.* work[12] shown in Figure S5, showing a similar trend for the cases of ethanol and acetonitrile. However, the rate differences in the methanol case indicate that the concentration of residual base in the methanol was changed by different dilution ratios with water, affecting the measured rates in Watarai *et al.* work. The strong catalytic effect of bases in solvents other than water highlights the need for caution when measuring intrinsic rates, particularly if the solutions were not neutralized.

AA tautomerization in mixtures of CD_3CN and D_2O is also studied using NMR, and the effect of water in mixtures of CH_3CN and H_2O is found to be similar to that in CD_3CN and D_2O (see Figure 13(b)). Note that the differences in tautomerization rates between H_2O and D_2O ($X_s = 0$) indicate the presence of isotope effect, which will be discussed in **section 3.6**.

3.5.2 Quantification

To compare the catalytic effects of water and base on the AA tautomerization rate, the data from Figure 13 were replotted using water concentration as the unit, shown in Figure 14. The reaction orders of water concentration fitted with (E10) are 1.22, 1.28, and 3.40 for methanol, ethanol, and acetonitrile, respectively.

$$k_{\mathrm{obs}} = k_0 + k_{\mathrm{W}}[\mathrm{H_2O}]^n \quad \text{(E10)}$$

where k_0 is the extrapolated rate of AA tautomerization in solvents without water in the unit of s^{-1}; k_W is the water catalytic effect in the unit of $s^{-1}\,M^{-n}$. n is the reaction order of water molar concentration. Similar to a result in Figure 11, the reaction order of water concentration demonstrates that water catalysis may undergo a multi-step process.

The linear fits are also applied for $[H_2O] < 15$ M, giving k_W of $(1.31 \pm 0.16)\times10^{-3}$, $(1.71 \pm 0.20)\times10^{-3}$, and $(1.69 \pm 0.58)\times10^{-4}$ s^{-1} M^{-1} (± 1 SD) for methanol, ethanol, and

doi:10.6342/NTU202503041

acetonitrile, respectively. The results reveal that water catalyzes 10^5 times weaker than base though its concentration is 10^5 times higher than base with a complementary direction, implying both factors are not ignorable in water system.

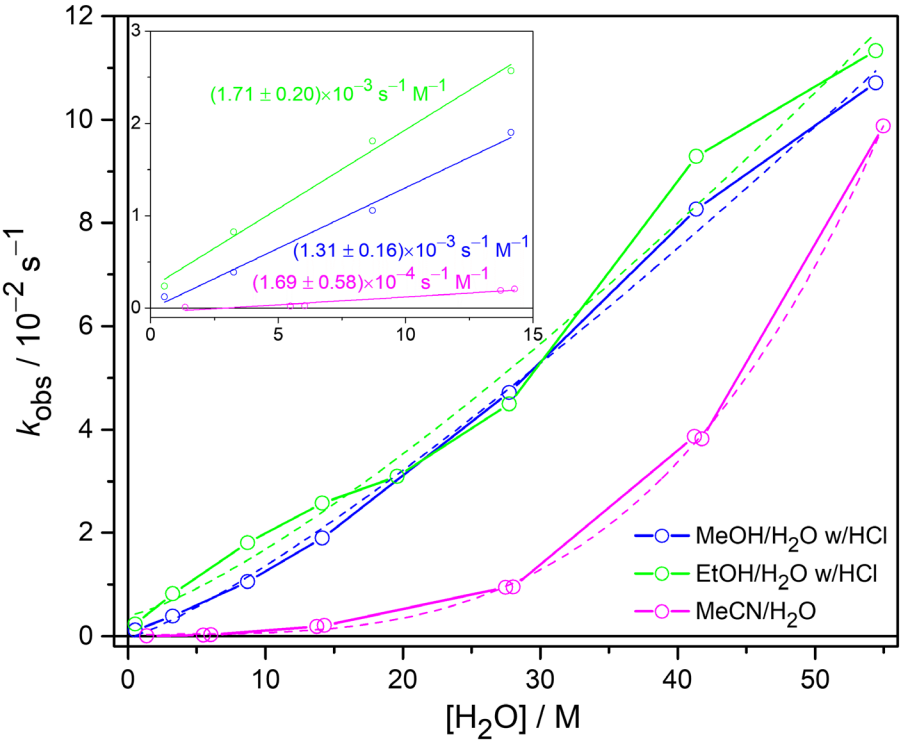

Figure 14 The effect of water concentrations to the tautomerization rates in organic solvents.

The dashed lines are power fits described by (E10), giving reaction orders of water concentration of 1.22, 1.28, and 3.40 for methanol, ethanol, and acetonitrile, respectively. For [H_2O] < 15 M shown in the enlarge, linear fits (solid lines) are attempted, giving k_W of $(1.31 \pm 0.16)\times10^{-3}$, $(1.71 \pm 0.20)\times10^{-3}$, and $(1.69 \pm 0.58)\times10^{-4}$ s^{-1} M^{-1} (± 1 SD) for methanol, ethanol, and acetonitrile, respectively. Same data as Figure 13.

doi:10.6342/NTU202503041

3.5.3 Proton-hopping mechanism

Several computational works show the intermediate structures of AA interacted with solvents in the tautomerization.[30-33] Yamabe *et al.* stated that the tautomerization was hard to break the C-H bond energy of AA keto form (87.6 kcal/mol), the hydrogen-bond network formed by water molecules was required to catalyze the tautomerization.[31] They also found a reaction of AA with two reactive and two catalytic water molecules (2+2) gave a small activation energy (15.27 kcal/mol), allowing an easy proton relay. Alagona *et al.* demonstrated the intramolecular hydrogen-bond formed by two water molecules in keto and enol forms of AA.[30] In addition, Watarai *et al.* proposed a tautomerization mechanism with the solvated ion pair formed as an intermediate, favoring the proton transfer between AA and solvents molecules.[12] Therefore, the solvent bridge was referred as the hydrogen-bonding in AA, catalyzing the tautomerization by the proton relay mechanism[34] (proton-hopping mechanism).

This study confirms the observation that AA itself undergoes tautomerization with difficulty, as demonstrated by the extremely slow rate observed in neutralized acetonitrile (see **section 3.4**). As an aprotic solvent lacking transferable protons, acetonitrile weakly catalyzes the tautomerization, consistent with the proton relay mechanism.

The fact that AA tautomerizes 90 times faster in water than in alcohols can be explained by differences in the solvents' acid strength.[12] It is reflected in the autoprotolysis constants of water and methanol (14 and 16.7, respectively),[35, 36] indicating a higher concentration of transferable protons in water. Although tautomerization rates are influenced by other factors such as ability of forming hydrogen-bond, it supports the proton relay mechanism as a plausible explanation.

doi:10.6342/NTU202503041

3.6 Kinetic isotope effect (KIE)

The kinetic isotope effects (KIE) of AA tautomerization in water and methanol were investigated with combinations of normal and d-solvents, as measured by UV absorption spectroscopy and shown in Figure 15 and Figure 16. As mentioned in **section 3.4**, HCL was added to neutralize the possible residual base in the methanol. The results reveal that the tautomerization follows the first-order kinetics described by E4 if isotope exchange is not involved. Quantitatively, the KIE is defined as below equation.

$$\text{Kinetic isotope effect (KIE)} = \frac{k_{\mathrm{H}}}{k_{\mathrm{D}}} \qquad \text{(E11)}$$

where k_{H} and k_{D} are the observed rate constants of tautomerization between normal solvents and d-solvents, respectively. As a result, KIE of tautomerization in water and methanol are determined to be 6.15 ± 0.39 and 6.35 ± 0.17 (± 1 SD), respectively. Similarly, Bell found the KIE of enolization of AA is 4.5.[37] Williams *et al.* found that the KIE of the enolization of malonamide ($CH_2(CONH_2)_2$) in sulfuric acid water solution is 2.2-2.3 by UV absorption spectroscopy.[38] Toullec *et al.* discussed the mechanism of acid-catalyzed enolization of acetone and reported a primary KIE ($k_{\mathrm{H}}/k_{\mathrm{D}}$) of enolization of 6.7 in sulfuric acid water solution, attributing it to the cleavage of the α (C–H or C–D) bond, which was identified as the rate-determining step (RDS) in the enolization of acetone.[39] Accordingly, the primary KIE of the AA tautomerization is also assumed to arise from the C–H bond breaking, suggesting that this step is the RDS in the tautomerization. In addition, the similar KIE values observed for AA tautomerization in water and methanol indicate that these two solvents play a minor role in the bond breaking mechanism.

doi:10.6342/NTU202503041

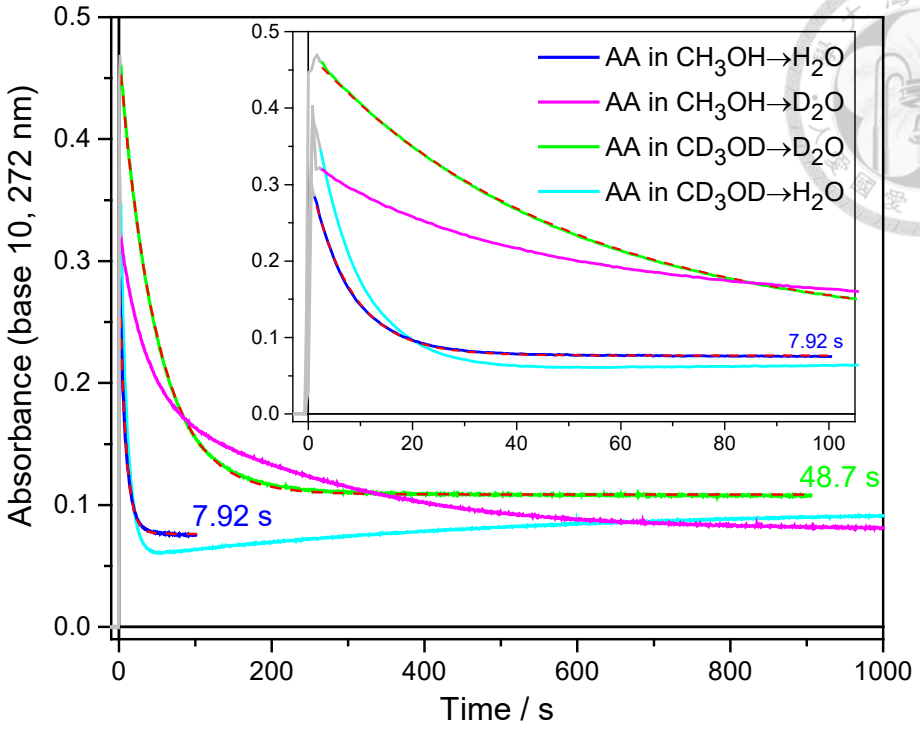

Figure 15 Time profiles of AA in H/D methanol mixed with H/D water in UV experiments.

Experimental conditions: [AA]: 4.67×10^{-5} M; $T = 25.4$°C. The dashed lines are first-order fits of (E5), giving lifetimes of 7.92 ± 0.41 and 48.70 ± 1.76 s for AA in $CH_3OH \rightarrow H_2O$ and AA in $CD_3OD \rightarrow D_2O$, respectively. The gray lines indicate the solutions were still mixing ca. 3 s. The KIE (k_H/k_D) is given as 6.15 ± 0.39 for AA tautomerization in water. Note that the profiles follow non-exponential behaviors if isotope exchange were involved, especially for the case of AA in $CD_3OD \rightarrow H_2O$, showing a reversion for the enol form.

doi:10.6342/NTU202503041

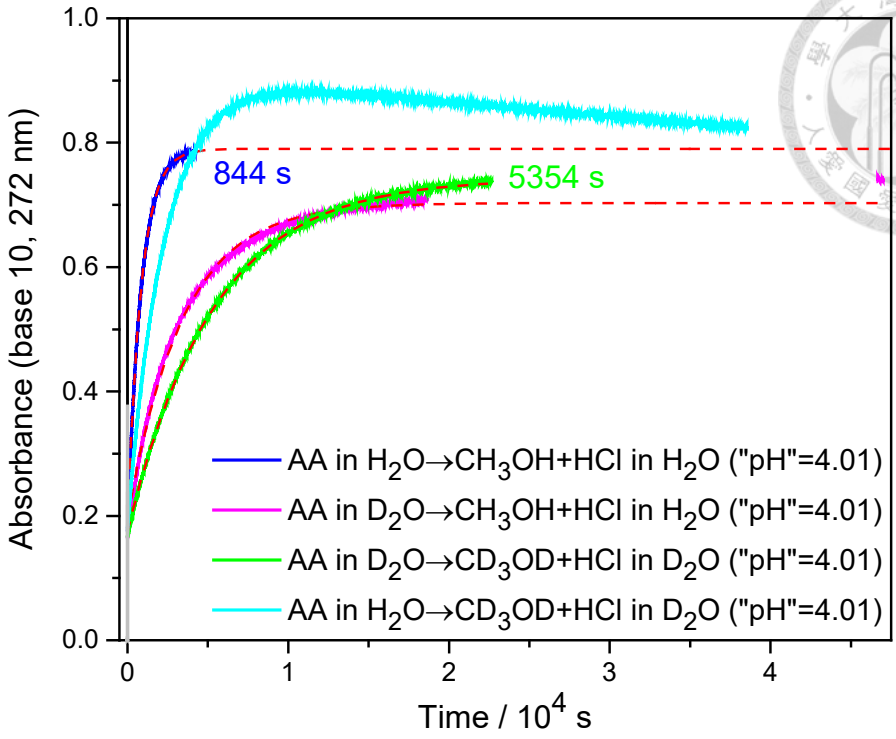

Figure 16 Time profiles of AA in H/D water mixed with H/D methanol in UV experiments.

Experimental conditions: [AA]: 9.90×10^{-5} M; [HCL]: 9.85×10^{-5} M; $T = 24.9$°C. pH values are assumed that the K_a of HCL in methanol is the same as that in water. The dashed lines are first-order fits of (E5), giving lifetimes of 844 and 5364 s for AA in $H_2O \rightarrow CH_3OH$ and AA in $D_2O \rightarrow CD_3OD$, respectively. The gray lines indicate the solutions were still mixing ca. 3 s. The KIE (k_H/k_D) is given as 6.35 ± 0.17 for AA tautomerization in methanol. Note that the profiles follow non-exponential behaviors if isotope exchange were involved, especially for the case of AA in $H_2O \rightarrow CD_3OD$, showing a reversion for the enol form.

3.6.1 Mechanism 1 simulation and Monte Carlo method

3.6.1.1 AA tautomerization in CD_3OD

To obtain a comprehensive view of AA tautomerization, ^{1}H pseudo-2D (intensity

doi:10.6342/NTU202503041

vs. chemical shift and time) NMR was employed to monitor the profiles of both enol and keto forms. Figure 17 shows time profiles of AA tautomerization in CD_3OD obtained by the NMR. The concentration fractions were calculated from following equations, and spectra are shown in Figure S6. Since fully-deuterated species will not be observed in ^1H spectra, enol 1D and keto 2D were obtained by (E13) and (E14), respectively.

$$\text{Concentration fraction} = \frac{[\text{AA peak}]}{[\text{Enol 6H}] + [\text{Keto 6H}]} \quad \text{(E12)}$$

$$\text{Concentration fraction of Enol 1D} = \text{Enol 6H} - \text{Enol 1H} \quad \text{(E13)}$$

$$\text{Concentration fraction of Keto 2D} = \text{Keto 6H} - \text{Keto 2H} - \text{Keto HD} \quad \text{(E14)}$$

$$\text{Transferable } \frac{\text{H}}{\text{D}} = \frac{[\text{Enol 1H}]_{\text{eq}} + [\text{Keto HD}]_{\text{eq}} + 2[\text{Keto 2H}]_{\text{eq}}}{[\text{Enol 1D}]_{\text{eq}} + [\text{Keto HD}]_{\text{eq}} + 2[\text{Keto 2D}]_{\text{eq}}} \quad \text{(E15)}$$

The pattern of enol 6H (green line) in Figure 17 is similar to that in UV results (Figure 16 cyan line), showing the non-exponential behaviors. Nichols *et al.* did the same experiment using a 300 MHz NMR, and they proposed a mechanism which fit their data well.[22] To analyze their data, they simplified the mechanism (ignore the k_{-2} and k_{-3} in mechanism 1, shown in Figure 3) due to the large excess of CD_3OD (transferable H/D: 3.09×10^{-2}, calculated from (E15)). However, the low transferable H/D would give small k_{-3} but not related to k_{-2}, which cannot explain the trend of AA peaks observed in our work, especially for those having a reversion in the beginning of the experiment.

Here, the mechanism 1 shown in Figure 3 is used to simulate the kinetics, and the results of global fits are summarized as Exp #2 in Table 4 and Table 5. The assumptions for the mechanism 1 are briefly listed below:

1. The tautomerization is accompanied by the isotope exchange.

2. The exchange rate between OH and OD in the enol form is assumed to be much faster than all the other reactions' rates,[22] also supported by the large full width at half maximum

doi:10.6342/NTU202503041

(FWHM) of the OH peak which is ca. 70 Hz in the low content of transferable deuterium experiment shown in Figure S7.

3. All the reactions are reversible.

As shown in Figure 17, the simulation curves (dashed lines) fit the overall time profiles well. However, relative deviations are larger for peaks with lower concentration fractions, likely due to poor fitting at low signal levels, especially for overlapping peaks under low magnetic field conditions. The relative errors of rate constants within 1 SD are summarized in Table 4, revealing that some variables are more insensitive than others. Therefore, we defined a variable as insensitive if the relative error exceeds 50% within 1 SD.

doi:10.6342/NTU202503041

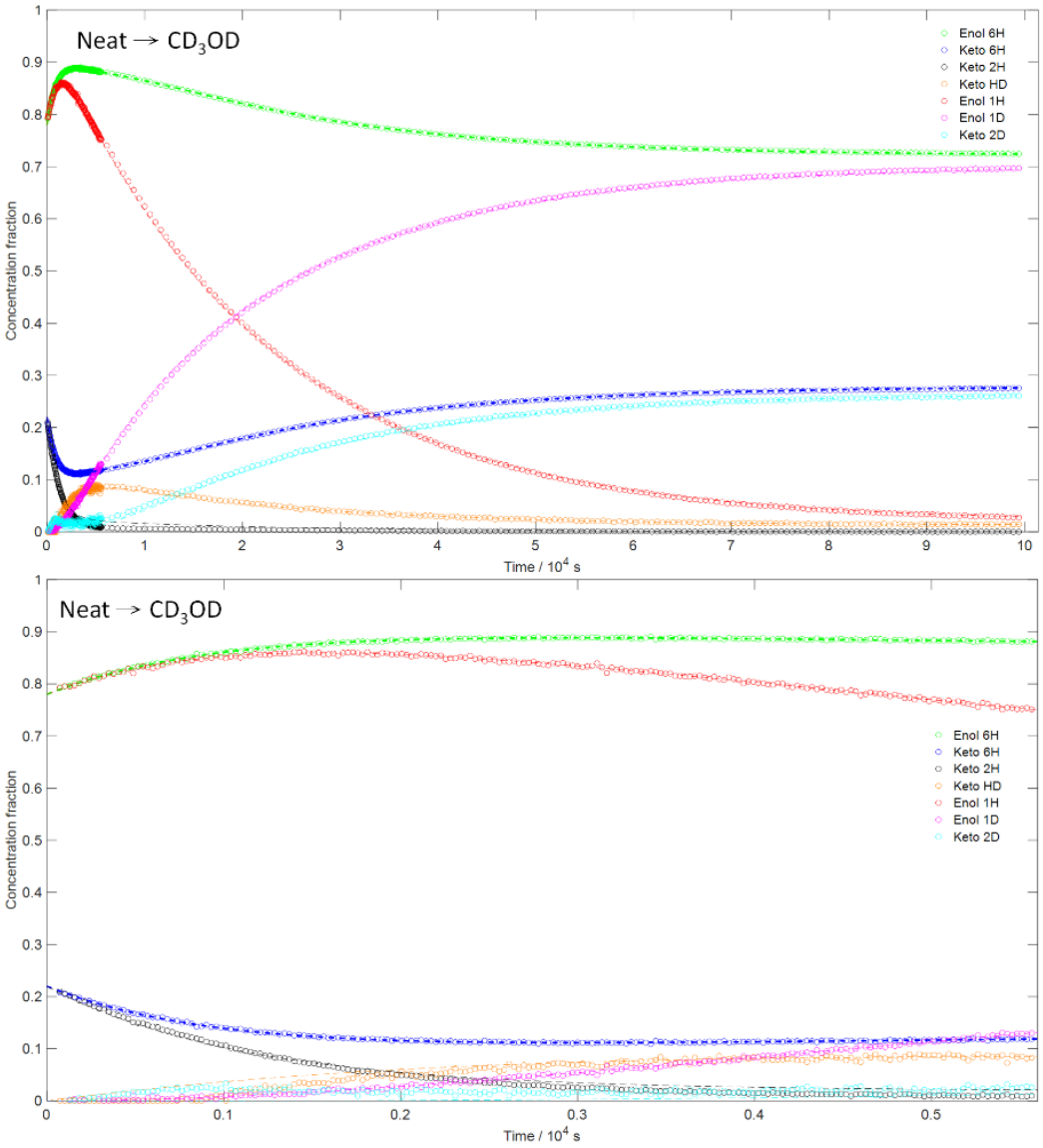

Figure 17 Time profiles (upper panel) and the enlarge (lower panel) of neat AA tautomerization in CD_3OD.

Experimental conditions: [AA]: 0.16 M; T = 25.0°C; ns: 1 for first 200 points and 20 for the others. The results are summarized as Exp #2 in Table 4 and Table 5. Hollow circles are the measured concentration fractions of the corresponding AA peaks, and dashed lines are global fits based on mechanism 1 shown in Figure 3. Enol 1D (magenta) and keto 2D (cyan) are calculated from (E13) and (E14), respectively. Note that the initial fraction of enol 1H was revised, as its fraction was approximately 5% higher than that

doi:10.6342/NTU202503041

of enol 6H, complicating the model simulation. The raw data are shown in Figure S8 for comparison.

Table 4 Exp #2 global fits' rates

Data points: 370; $K_{eq,1–4}$: 40.397, 0.680, 53.936, 0.378

Rate / s^{-1}	Keto 2H → Enol 1H (k_1)	Enol 1H → Keto HD (k_2)	Keto HD → Enol 1D (k_3)	Enol 1D → Keto 2D (k_4)	Initial keto fraction
Min[a]	7.81×10^{-4}	5.15×10^{-5}	3.73×10^{-4}	4.29×10^{-5}	0.206
Best fit	8.89×10^{-4}	5.62×10^{-5}	4.20×10^{-4}	5.29×10^{-5}	0.220
Max[a]	9.95×10^{-4}	6.07×10^{-5}	4.73×10^{-4}	7.53×10^{-5}	0.235
Error	± 12%	± 8%	± 12%	−19% +42%	± 6%

a One standard deviation

Water was also selected as an alternative solvent 1 to initiate the tautomerization with a lower enol fraction. The results of global fits are summarized as Exp #3 in Table 5, while the corresponding spectra and time profiles are shown in Figure S9 and Figure S10, respectively. In summary, mechanism 1 is applicable with water as solvent 1, yielding an initial enol fraction of 0.21, comparable to the reported value of 0.19 in water.[23] The rates are faster than those observed in Exp #2, likely due to the higher water concentration and the larger transferable H/D.

3.6.1.2 Simulation of other solvents — D_2O catalytic effect

The mechanism 1 were also applied for AA tautomerization in D_2O and the mixtures of CD_3CN/D_2O. The results of global fits are summarized as Exp #1, 4–6 in Table 6, respectively. The corresponding spectra and time profiles are shown in Figure S2, and Figure S11–Figure S17. As shown in Figure 18, tautomerization rates of Exp #1, 4–6 are plotted against D_2O concentration. Similar to the results discussed in **section 3.5.2**, D_2O also catalyzed the tautomerization in CD_3CN. The reaction orders of D_2O concentration for k_2–k_4 and k_{-2}–k_{-4} fitted by (E10) are 3.01, 2.32, 4.63, 1.29, 5.34, and

doi:10.6342/NTU202503041

2.93, respectively. Here, k_1 and k_{-1} were not fitted due to their insensitivity (relative error within 1 SD > 50%) in Exp #1, 4–5. As a result, the non-first reaction orders of D_2O concentration indicate D_2O catalyzes the tautomerization through a multi-step process, which differs when isotope exchange is involved.

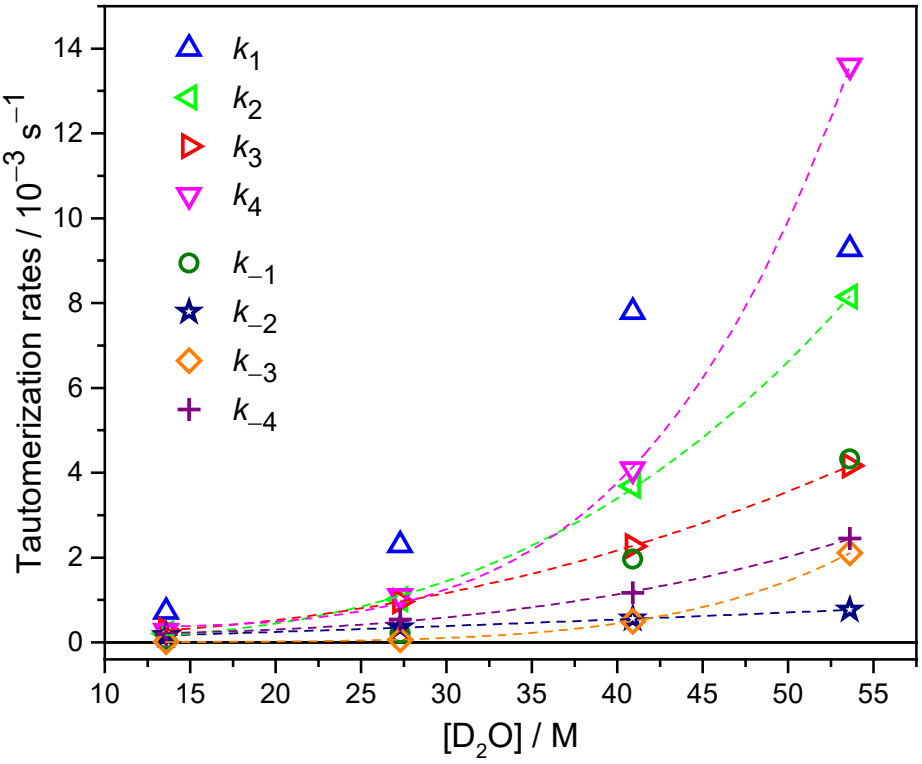

Figure 18 The effect of D_2O concentrations to the tautomerization rates in CD_3CN.

The hollow symbols represent the rates summarized in Table 6, obtained by fitting the time profiles using mechanism 1. The dashed lines are power fits described by (E10), giving reaction orders of D_2O concentration of 3.01, 2.32, 4.63, 1.29, 5.34, and 2.93 for k_2–k_4 and k_{-2}–k_{-4}, respectively. Here, k_1 and k_{-1} were not fitted due to their insensitivity (relative error within 1 SD > 50%).

doi:10.6342/NTU202503041

Table 5 Conditions and results of AA tautomerization in D_2O and CD_3OD.

The experiments were conducted in the 80 MHz NMR; T = 25.0°C.

Here, rate constants were obtained by simulating mechanism 1, shown in Figure 3.

Exp #	Solvent 1	Solvent 2	[AA] / M	[b]Trans-ferable H / D	k_1 / s^{-1}	k_2 / s^{-1}	k_3 / s^{-1}	k_4 / s^{-1}	k_{-1} / s^{-1}	k_{-2} / s^{-1}	k_{-3} / s^{-1}	k_{-4} / s^{-1}	Initial keto fraction
1	Neat	D_2O	0.32	0.047	[a]9.27×10^{-3}	8.15×10^{-3}	4.17×10^{-3}	1.36×10^{-2}	[a]4.32×10^{-3}	7.69×10^{-4}	2.11×10^{-3}	2.45×10^{-3}	[a]0.050
2	Neat	CD_3OD	0.16	0.027	8.89×10^{-4}	5.62×10^{-5}	4.20×10^{-4}	5.29×10^{-5}	2.20×10^{-5}	8.26×10^{-5}	7.79×10^{-6}	1.40×10^{-4}	0.220
3	H_2O	CD_3OD	0.046	0.17	1.36×10^{-3}	1.06×10^{-4}	6.48×10^{-4}	[a]1.28×10^{-4}	1.02×10^{-4}	1.60×10^{-4}	7.51×10^{-5}	[a]3.41×10^{-4}	0.786

a. Insensitive variables (relative error with 1 SD > 50%)

b. Calculated from (E15)

Table 6 Conditions and results of AA tautomerization in different fractions of CD_3CN and D_2O.

The experiments were conducted in the 80 MHz NMR; T = 25.0°C.

Here, rate constants were obtained by simulating mechanism 1, shown in Figure 3.

Exp #	Solvent 1	Solvent 2	[AA] / M	[D_2O] / M	[b]Trans-ferable H / D	k_1 / s^{-1}	k_2 / s^{-1}	k_3 / s^{-1}	k_4 / s^{-1}	k_{-1} / s^{-1}	k_{-2} / s^{-1}	k_{-3} / s^{-1}	k_{-4} / s^{-1}	Initial keto fraction
1	Neat	D_2O	0.32	53.6	0.047	[a]9.27×10^{-3}	8.15×10^{-3}	4.17×10^{-3}	1.36×10^{-2}	[a]4.32×10^{-3}	7.69×10^{-4}	2.11×10^{-3}	2.45×10^{-3}	[a]0.050
4	Neat	CD_3CN +D_2O	0.16	40.9	0.033	[a]7.79×10^{-3}	3.69×10^{-3}	2.27×10^{-3}	4.08×10^{-3}	[a]1.96×10^{-3}	5.56×10^{-4}	4.99×10^{-4}	1.17×10^{-3}	[a]0.136
5	Neat	CD_3CN +D_2O	0.16	27.3	0.019	[a]2.29×10^{-3}	1.01×10^{-3}	9.72×10^{-4}	1.09×10^{-3}	[a]2.08×10^{-4}	3.48×10^{-4}	6.54×10^{-5}	5.44×10^{-4}	0.206
6	Neat	CD_3CN +D_2O	0.16	13.6	0.031	7.21×10^{-4}	2.09×10^{-4}	2.80×10^{-4}	2.67×10^{-4}	6.74×10^{-5}	1.68×10^{-4}	1.94×10^{-5}	1.94×10^{-4}	0.215

a. Insensitive variables (relative error with 1 SD > 50%)

b. Calculated from (E15)

3.6.1.3 Variable pairs fitting

The relationships of each pair of variables were investigated by fitting the mechanism 1 while keeping the other variables fixed at the best-fit values obtained from the global fits. As shown in Figure 19, some variable pairs in the fitting of Exp #2 exhibit correlation, as indicated by the oblique elliptical shapes. These results highlight the challenges of multi-variable fitting, particularly for insensitive variables. Additional boundary conditions, beyond total concentration and equilibrium constants, are required to achieve more reliable quantifications. Besides that, mechanism 1, qualitatively and semi-quantitatively explains AA tautomerization in the absence of base.

Variable pairs fittings obtained from other experiments are summarized in Figure S18–Figure S22. Due to the insensitivity of certain variables, the elliptical shapes appear distorted and their error boundaries are difficult to fit.

doi:10.6342/NTU202503041

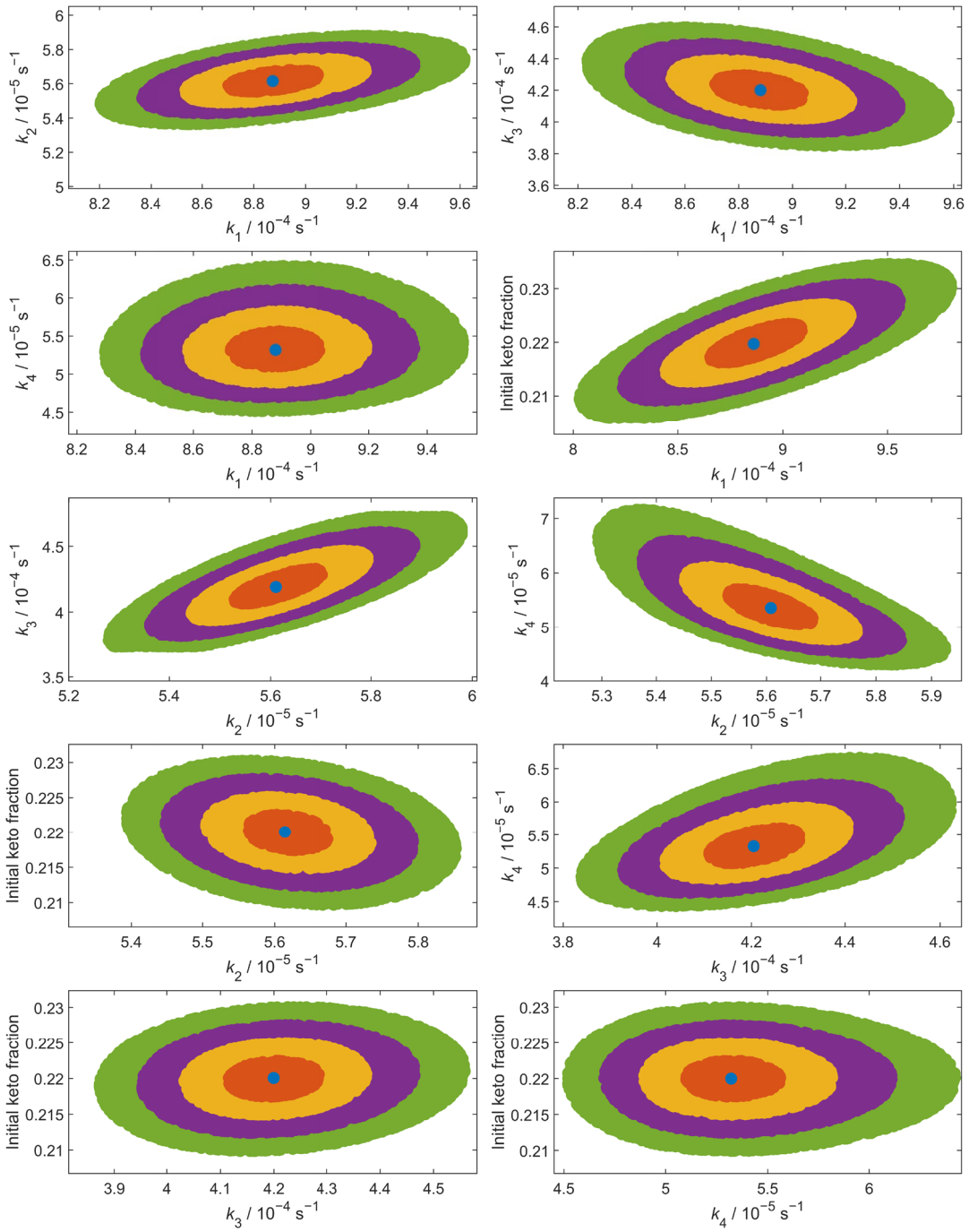

Figure 19 Fits of two variables in Exp #2.

The remaining variables were fixed at the values obtained from global fits, as shown in Table 5. The blue, orange, yellow, purple, and green points correspond to errors of 0, 0.25, 0.5, 0.75, and 1 SD, respectively.

doi:10.6342/NTU202503041

3.6.1.4 Enolization and ketolization rates

To investigate the isotope effect and trend of the simulating rates listed in Table 5 and Table 6, they are distinguished into rates of enolization and ketolization. Enolization rates include k_1, k_3, k_{-2}, and k_{-4}, while ketolization rates include k_2, k_4, k_{-1}, and k_{-3}. Considering the isotope exchange in mechanism 1, trends are assumed as following

$$\text{Enolization: } k_1 \sim 2k_3 > k_{-4} \sim 2k_{-2} \qquad \text{(E16)}$$

$$\text{Ketolization: } k_2 \sim k_4 > k_{-1} > k_{-3} \qquad \text{(E17)}$$

Note that the transferable H/D is different among Exp #1-6, the rates are compared with those from similar reactions in the same experiment. As a result, the forward rate constants are higher than the reverse rate constants, likely due to the low content of transferable H/D.

In enolization reactions, the C–H (or C–D) bond is cleaved, and the resulting H (or D) is transferred via a solvent bridge, referring to the proton hopping mechanism, as discussed in **section 3.5.3**. By simply counting the number of C–H bonds, the cleavage probability of keto 2H (k_1) is twice as high as that of keto HD (k_3), leading to the formation of the corresponding enol species. Similarly, the C–D bond cleavage probability of keto 2D (k_{-4}) is also twice as high as that of keto HD (k_{-2}), as described in (E16).

In ketolization reactions, the C–H (or C–D) bonds are formed. Since transferable H/D is the same in the solution, the probabilities of bond formation are similar, resulting in similar rates for the k_2 and k_4. However, in environments with low ratios of transferable H/D, the formation of C–H bond is much rarer than that of C–D bond. The slow rates amplify the secondary isotope effect for the k_{-1} and k_{-3}, resulting a higher rate for k_{-1} forming C–H bond with an adjacent H, as described in (E17).

doi:10.6342/NTU202503041

3.6.1.5 KIE

The ratios of rates are further summarized in Table 7 to investigate the relationships. In enolization reactions, the rate ratios of k_1/k_3 = 1.20–3.09; k_{-4}/k_{-2} = 1.23–2.80 indicate the probability ratio of the cleavage of C–H (or C–D) bond, respectively, as discussed in previous section. In addition, KIEs of tautomerization in D_2O, CD_3OD, and CD_3CN are represented by the rate ratios of k_3/k_{-2} with values of 3.76–7.74, 4.17–6.24, and 1.22–2.36, respectively. Similarly, KIE of tautomerization in CD_3OD is also obtained by k_1/k_{-4} with value of 3.92–8.77. In summary, KIEs of tautomerization in D_2O and CD_3OD obtained from NMR experiments are comparable to those determined by UV experiments (6.15 ± 0.39 and 6.35 ± 0.17 for water and methanol, respectively).

In ketolization reactions, the rate ratios of k_4/k_2 = 0.85–1.48; k_{-1}/k_{-3} = 0.78–3.56 indicate the probability ratio of the formation of C–D (or C–H) bond, respectively, as discussed in previous section. Note that the larger value of k_{-1}/k_{-3} may indicate the secondary KIE observed in C–H bond formation.

doi:10.6342/NTU202503041

Table 7 Conditions and rate ratios of Exp #1–6

The experiments were conducted in the 80 MHz NMR; T = 25.0°C. Rate constants were obtained by simulating mechanism 1

The values in parentheses indicate unreliable determination, with relative errors > 50% within 1 SD

Exp #	Solvent 1	Solvent 2	[D_2O] / M	[a]Transferable H/D	k_1 / k_3	k_{-4} / k_{-2}	k_3 / k_{-2}	k_1 / k_{-4}	k_4 / k_2	k_{-1} / k_{-3}
1	Neat	D_2O	53.6	0.047	$(2.22^{+2.72}_{-1.34})$	$(3.19^{+1.82}_{-1.00})$	$5.42^{+2.32}_{-1.66}$	$(3.78^{+4.72}_{-2.42})$	$(1.67^{+0.96}_{-0.52})$	$(2.05^{+2.51}_{-1.23})$
2	Neat	CD_3OD		0.027	$2.12^{+0.55}_{-0.47}$	$(1.69^{+0.94}_{-0.42})$	$5.08^{+1.16}_{-0.91}$	$6.35^{+2.42}_{-2.43}$	$(0.94^{+0.52}_{-0.23})$	$2.82^{+0.74}_{-0.62}$
3	H_2O	CD_3OD		0.17	$2.10^{+0.99}_{-0.90}$	$(2.13^{+5.95}_{-1.11})$	$(4.05^{+3.83}_{-1.61})$	$(3.99^{+3.39}_{-2.82})$	$(1.21^{+3.38}_{-0.63})$	$1.36^{+0.64}_{-0.58}$
4	Neat	CD_3CN +D_2O	40.9	0.033	$(3.43^{+15.46}_{-2.51})$	$2.10^{+0.70}_{-0.51}$	$4.08^{+1.56}_{-1.08}$	$(6.66^{+28.83}_{-4.80})$	$1.11^{+0.37}_{-0.26}$	$(3.93^{+17.72}_{-2.87})$
5	Neat	CD_3CN +D_2O	27.3	0.019	$(2.36^{+2.46}_{-1.23})$	$1.56^{+0.46}_{-0.33}$	$2.79^{+0.82}_{-0.54}$	$(4.21^{+4.59}_{-2.21})$	$1.08^{+0.32}_{-0.23}$	$(3.18^{+3.31}_{-1.67})$
6	Neat	CD_3CN +D_2O	13.6	0.031	$(2.58^{+2.34}_{-1.25})$	$(1.15^{+0.79}_{-0.38})$	$1.67^{+0.69}_{-0.45}$	$(3.72^{+4.01}_{-2.12})$	$(1.28^{+0.88}_{-0.42})$	$(3.47^{+3.17}_{-1.68})$

a. Calculated from (E15)

3.6.2 Mechanism 2 simulating — base catalytic effect

The base catalytic effect is further confirmed by comparing the rates shown in Figure 20 and Figure 21 which demonstrate that [NaOD] of 4.31 μM catalyzes the tautomerization at least five times faster than the experiment without added base. The time profiles shown in Figure 21 were also fitted using mechanism 1 (dotted lines), but the fits were notably worse compared to the previous results without adding base.

To investigate the base-involved mechanism, proton abstraction—as illustrated in Figure 9—is assumed to participate in the tautomerization, with the enolate/anionic form acting as an intermediate. The enolate intermediate enables an alternative pathway for isotope exchange, catalyzing reactions between the keto forms. It explains the initially faster rate of keto 2H in tautomerization, as shown in Figure 21. Therefore, mechanism 2 shown in Figure 4 was proposed to fit the tautomerization in the presence of added base, with the resulting rates summarized as Exp #8 in Table 8.

As shown in Figure 21, the global fits using mechanism 2 (Exp #8-1, dashed lines) demonstrate a better match than those from mechanism 1 (Exp #8-3, dotted lines), particularly for the keto 2H profile which is sensitive to the rate of isotope exchange. However, the initial keto fraction of Exp #8-1 is ca. 24% lower than those observed in experiments using the same solvent 1. To enable rate comparison, mechanism 2 was also fitted with the initial keto fraction fixed at 0.21, and the results are summarized as Exp #8-2 (dashed-dotted lines).

Though the rate differences between two mechanism 2 fits are not significant, the superior simulation profiles of mechanism 2 relative to mechanism 1 support the proposed enolate-catalyzed pathway for tautomerization under base-added conditions.

doi:10.6342/NTU202503041

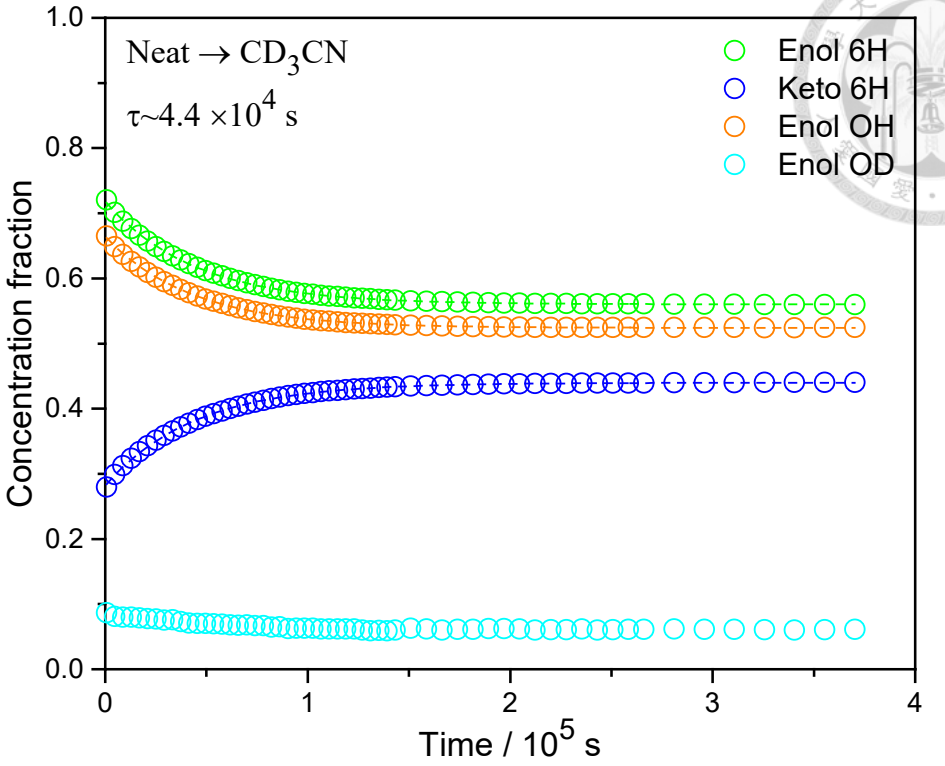

Figure 20 Time profiles of neat AA tautomerization in CD_3CN.

Experimental conditions: [AA]: 0.16 M; T = 25.0°C; ns: 16 and delay time: 25 s for all the points. The results are summarized as Exp #7 in Table 8. The spectra are shown in Figure S23. Hollow circles are the measured concentration fractions of the corresponding AA peaks, and dashed lines are first-order fits of (E5), giving the lifetime of ca. 4.4×10^4 s.

doi:10.6342/NTU202503041

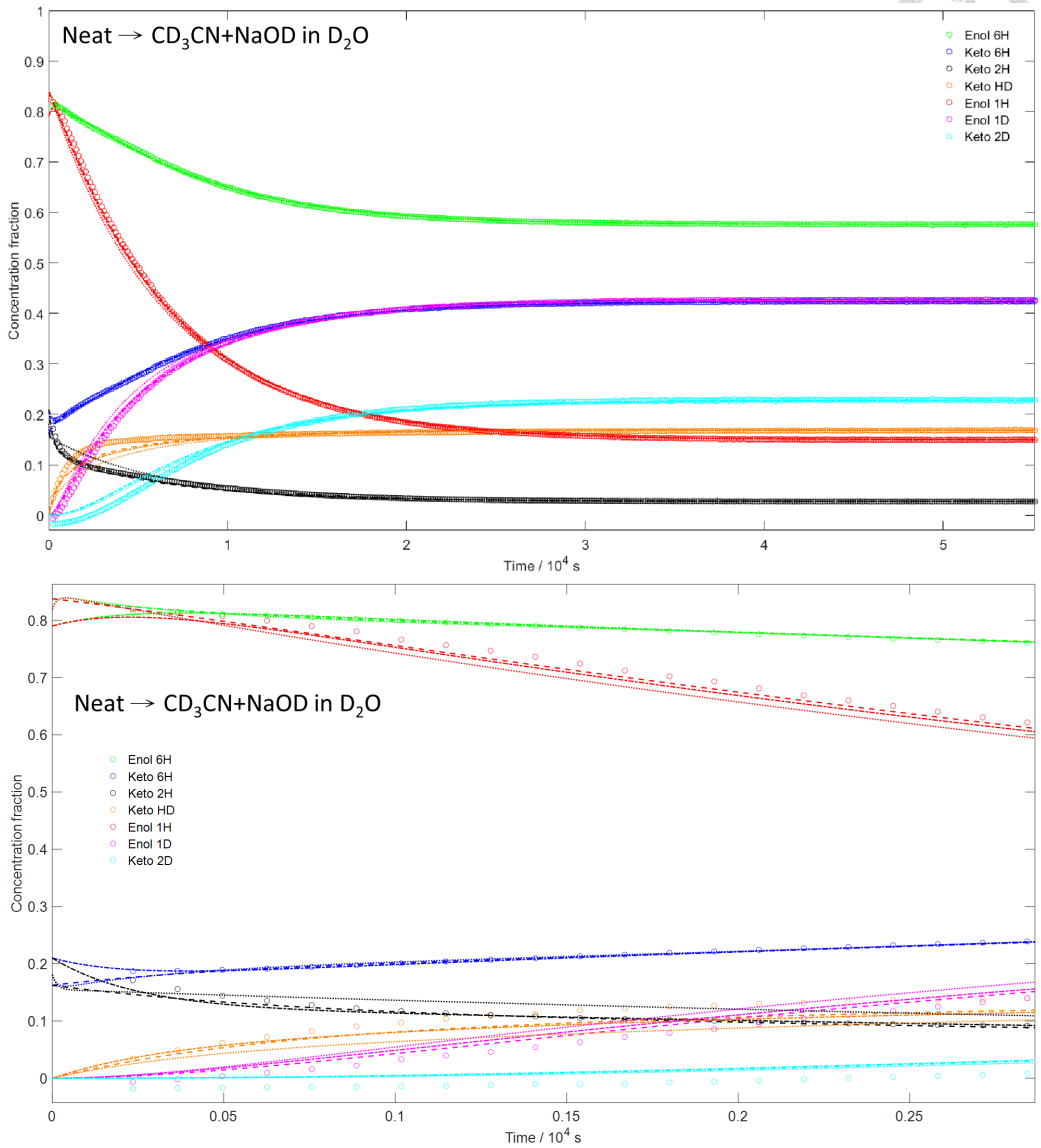

Figure 21 Time profiles (upper panel) and the enlarge (lower panel) of neat AA tautomerization in CD_3CN+NaOD in D_2O.

Experimental conditions: [AA]: 0.16 M; [NaOD]: 4.31×10^{-6} M; [D_2O]: 0.54 M; T = 25.0°C; ns: 8 and delay time: 15 s for all the points. The results are summarized as Exp #8 in Table 8. The spectra are shown in Figure S24. Hollow circles are the measured concentration fractions of the corresponding AA peaks. Dashed lines (Exp #8-1) are global fits based on mechanism 2; dashed-dotted lines (Exp #8-2) follow the same fitting procedure as the dashed lines but with the initial keto fraction fixed at 0.21; dotted lines (Exp #8-3) are global fits based on mechanism 1.

doi:10.6342/NTU202503041

doi:10.6342/NTU202503041

Table 8 Conditions and results of AA tautomerization in CD_3CN+NaOD in D_2O.

The experiments were conducted in the 600 MHz NMR; T = 25.0°C.

Here, rate constants were obtained by simulating mechanism 2, shown in Figure 4.

[c]Exp #	Solvent 1	Solvent 2	[AA] / M	[NaOD] / M	[b]Transferable H / D	k_1 / s^{-1}	k_2 / s^{-1}	k_3 / s^{-1}	k_4 / s^{-1}	k_{B1} / s^{-1}	k_{B2} / s^{-1}	k_{-1} / s^{-1}	Initial keto fraction
7	Neat	CD_3CN	0.16	0	8.61	1.27×10^{-5}	--	--	--	--	--	1.00×10^{-5}	0.26
8-1	Neat	CD_3CN +NaOD in D_2O	0.16	4.31×10^{-6}	0.35	[a]8.58×10^{-4}	9.58×10^{-4}	1.06×10^{-3}	1.42×10^{-4}	4.36×10^{-4}	[a]4.46×10^{-5}	[a]1.57×10^{-4}	0.16
8-2	Same as above					[a]2.84×10^{-3}	2.96×10^{-5}	1.15×10^{-3}	1.37×10^{-4}	8.55×10^{-4}	[a]4.91×10^{-5}	[a]5.20×10^{-4}	0.21
8-3	Same as above					[a]6.98×10^{-2}	1.62×10^{-4}	1.85×10^{-3}	1.45×10^{-4}	--	--	[a]1.28×10^{-2}	[a]0.19

a. Insensitive variables (relative error with 0.5 SD > 50%)

b. Calculated from (E15)

c. Rates of #7 were obtained by fitting first-order kinetics (E5) of enol 6H;
Rates of #8-1 and #8-3 were obtained by global fits of mechanism 2 and 1, respectively.
Rates of #8-2 were obtained by simulating mechanism 2 with a fixed initial keto fraction of 0.21.
Equilibrium constants of #8, $K_{eq,1-4}$, $K_{eq,B1,B2}$: 5.464, 1.128, 2.534, 0.534, 6.162, 1.353, respectively.

Chapter 4 Conclusions

In this work, the catalytic effects of enol-keto tautomerization of AA in water, methanol, ethanol, acetonitrile, and their deuterated solvents were investigated. The results reveal that AA tautomerization follows first order kinetics when isotope exchange is not involved. The tautomerization rates of AA in solvents are water > alcohols > acetonitrile. In addition, base catalytic effects in CH_3CN and alcohols are determined to be 269 ± 106 and 1715 ± 195 s^{-1} M^{-1} (± 1 SD), respectively. Acid catalytic effects are insignificant in all studied solvents except in CH_3CN, where a weak catalytic effect of 4.19 ± 0.47 s^{-1} M^{-1} (± 1 SD) is observed. Water catalytic effects are approximately (1.69 ± 0.58)×10^{-4} and (1.53 ± 0.38)×10^{-3} s^{-1} M^{-1} (± 1 SD) in CH_3CN and alcohols, respectively. Kinetic isotope effects (KIEs, k_H/k_D) of AA tautomerization in water and methanol are determined to be 6.15 ± 0.39 and 6.35 ± 0.17 (± 1 SD), respectively, comparable to the reported KIE value of 4.5 for AA enolization.[37] In addition, two kinetic models were proposed to simulate the non-exponential concentration profiles under both base-free and base-catalyzed conditions. The results demonstrate that AA tautomerization and isotope exchange proceed concurrently, facilitated by both a solvent bridge and the enolate intermediate. Moreover, the enolate form enables isotope exchange in the absence of tautomerization. KIEs of AA tautomerization in D_2O and CD_3OD are also determined to be 3.76–7.74 and 3.92–8.77, respectively. In summary, this work provides deeper insight into the catalytic mechanisms of water and base, as well as their interplay with isotope exchange in AA tautomerization.

doi:10.6342/NTU202503041

Chapter 5 Supporting information

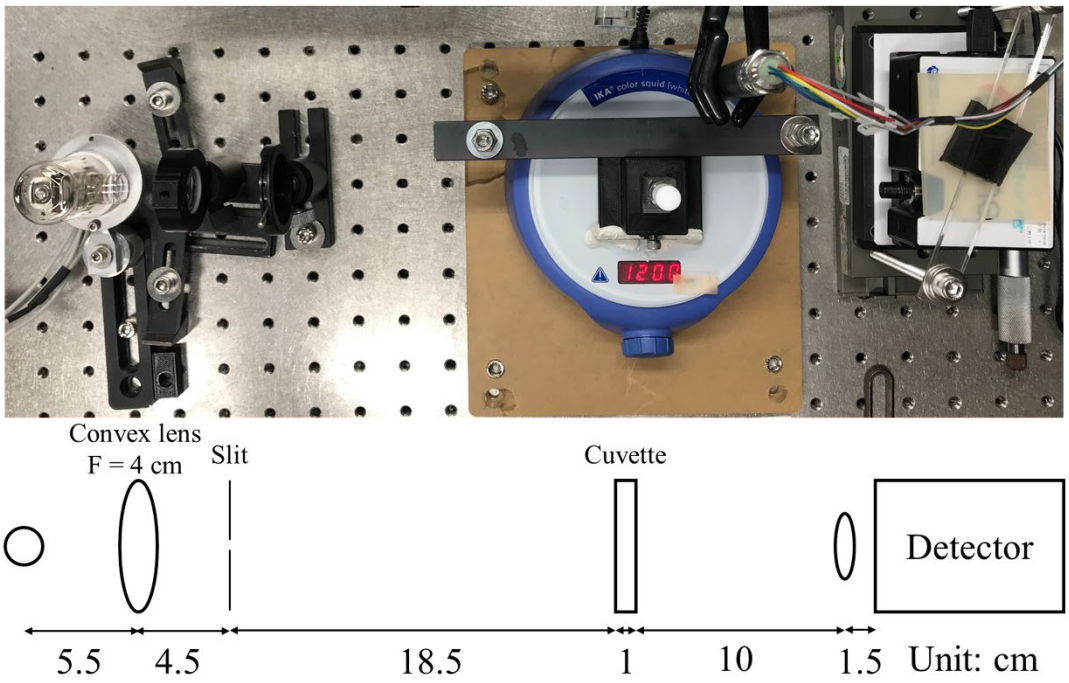

Figure S1 Picture of device of UV absorption spectroscopy.

A calibrated thermometer was positioned near the cuvette to monitor the temperature.

doi:10.6342/NTU202503041

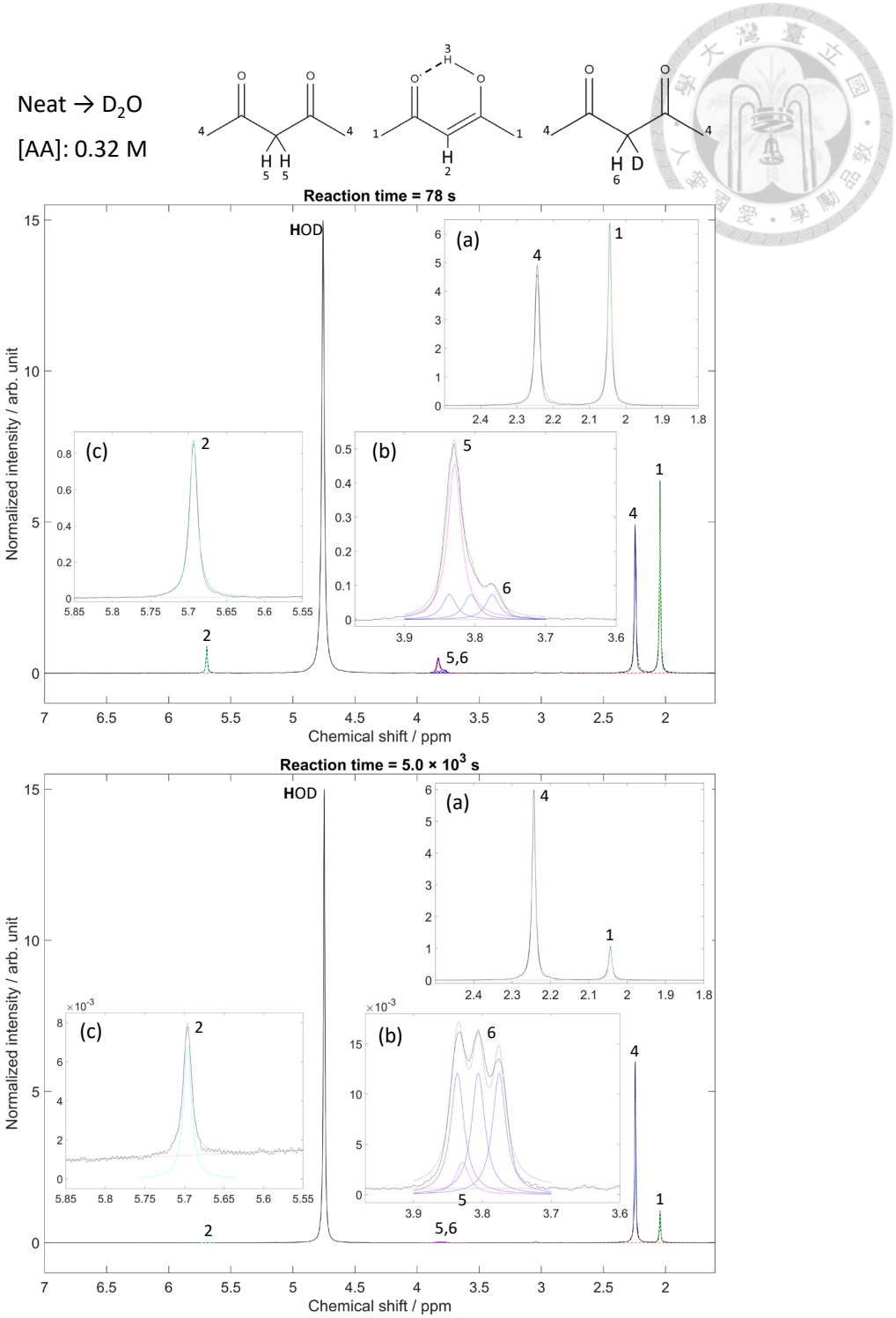

Figure S2 NMR spectrum of neat AA liquid in D_2O.

Experimental conditions: [AA]: 0.32 M, T = 25.0°C. Upper and lower panels are the spectrums at 78 and 5×10^3 s, respectively. The experiment was conducted at 80 MHz NMR, and peaks were referenced to enol 6H at 2.044 ppm. The red dashed lines are the linear baseline fits, and the colored lines are Lorentzian fits (E1).

doi:10.6342/NTU202503041

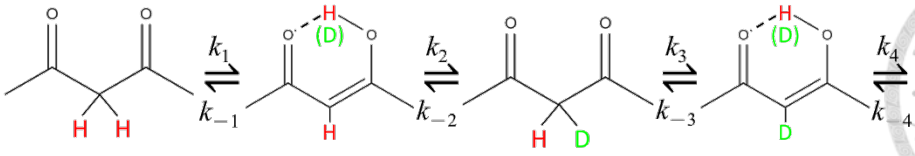

Rate equations

$$-\frac{\mathrm{d[Keto\ 2H]}}{\mathrm{d}t} = k_1[\mathrm{Keto\ 2H}] - k_{-1}[\mathrm{Enol\ 1H}]$$

$$-\frac{\mathrm{d[Enol\ 1H]}}{\mathrm{d}t} = -k_1[\mathrm{Keto\ 2H}] + (k_{-1}+k_2)[\mathrm{Enol\ 1H}] - k_{-2}[\mathrm{Keto\ HD}]$$

$$-\frac{\mathrm{d[Keto\ HD]}}{\mathrm{d}t} = -k_2[\mathrm{Enol\ 1H}] + (k_{-2}+k_3)[\mathrm{Keto\ HD}] - k_{-3}[\mathrm{Enol\ 1D}]$$

$$-\frac{\mathrm{d[Enol\ 1D]}}{\mathrm{d}t} = -k_3[\mathrm{Keto\ HD}] + (k_{-3}+k_4)[\mathrm{Enol\ 1D}] - k_{-4}[\mathrm{Keto\ 2D}]$$

$$\frac{\mathrm{d[Keto\ 2D]}}{\mathrm{d}t} = k_4[\mathrm{Enol\ 1D}] - k_{-4}[\mathrm{Keto\ 2D}]$$

Boundary conditions

$$[\mathrm{Keto\ 2H}] + [\mathrm{Keto\ HD}] + [\mathrm{Keto\ 2D}] = [\mathrm{Keto\ 6H}]$$

$$[\mathrm{Enol\ 1H}] + [\mathrm{Enol\ 1D}] = [\mathrm{Enol\ 6H}]$$

$$\frac{k_1}{k_{-1}} = \frac{[\mathrm{Enol\ 1H}]_{eq}}{[\mathrm{Keto\ 2H}]_{eq}} \qquad \frac{k_2}{k_{-2}} = \frac{[\mathrm{Keto\ HD}]_{eq}}{[\mathrm{Enol\ 1H}]_{eq}}$$

$$\frac{k_3}{k_{-3}} = \frac{[\mathrm{Enol\ 1D}]_{eq}}{[\mathrm{Keto\ HD}]_{eq}} \qquad \frac{k_4}{k_{-4}} = \frac{[\mathrm{Keto\ 2D}]_{eq}}{[\mathrm{Enol\ 1D}]_{eq}}$$

Figure S3 Rate equations and boundary conditions of mechanism 1.

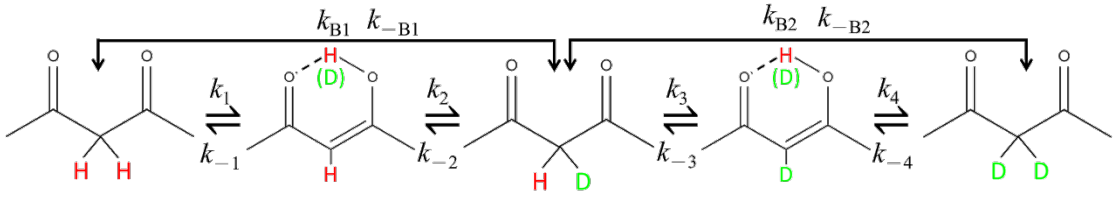

Rate equations

$$-\frac{\mathrm{d[Keto\ 2H]}}{\mathrm{d}t} = (k_1+k_{B1})[\mathrm{Keto\ 2H}] - k_{-1}[\mathrm{Enol\ 1H}] - k_{-B1}[\mathrm{Keto\ HD}]$$

$$-\frac{\mathrm{d[Enol\ 1H]}}{\mathrm{d}t} = -k_1[\mathrm{Keto\ 2H}] + (k_{-1}+k_2)[\mathrm{Enol\ 1H}] - k_{-2}[\mathrm{Keto\ HD}]$$

$$-\frac{\mathrm{d[Keto\ HD]}}{\mathrm{d}t} = -k_{B1}[\mathrm{Keto\ 2H}] - k_2[\mathrm{Enol\ 1H}] + (k_{-B1}+k_{-2}+k_3+k_{B2})[\mathrm{Keto\ HD}] - k_{-3}[\mathrm{Enol\ 1D}] - k_{-B2}[\mathrm{Keto\ 2D}]$$

$$-\frac{\mathrm{d[Enol\ 1D]}}{\mathrm{d}t} = -k_3[\mathrm{Keto\ HD}] + (k_{-3}+k_4)[\mathrm{Enol\ 1D}] - k_{-4}[\mathrm{Keto\ 2D}]$$

$$\frac{\mathrm{d[Keto\ 2D]}}{\mathrm{d}t} = k_{B2}[\mathrm{Keto\ HD}] + k_4[\mathrm{Enol\ 1D}] - (k_{-B2}+k_{-4})[\mathrm{Keto\ 2D}]$$

Boundary conditions

$$[\mathrm{Keto\ 2H}] + [\mathrm{Keto\ HD}] + [\mathrm{Keto\ 2D}] = [\mathrm{Keto\ 6H}]$$

$$[\mathrm{Enol\ 1H}] + [\mathrm{Enol\ 1D}] = [\mathrm{Enol\ 6H}]$$

$$\frac{k_1}{k_{-1}} = \frac{[\mathrm{Enol\ 1H}]_{eq}}{[\mathrm{Keto\ 2H}]_{eq}} \qquad \frac{k_{B1}}{k_{-B1}} = \frac{[\mathrm{Keto\ HD}]_{eq}}{[\mathrm{Keto\ 2H}]_{eq}}$$

$$\frac{k_2}{k_{-2}} = \frac{[\mathrm{Keto\ HD}]_{eq}}{[\mathrm{Enol\ 1H}]_{eq}} \qquad \frac{k_{B2}}{k_{-B2}} = \frac{[\mathrm{Keto\ 2D}]_{eq}}{[\mathrm{Keto\ HD}]_{eq}}$$

$$\frac{k_3}{k_{-3}} = \frac{[\mathrm{Enol\ 1D}]_{eq}}{[\mathrm{Keto\ HD}]_{eq}}$$

$$\frac{k_4}{k_{-4}} = \frac{[\mathrm{Keto\ 2D}]_{eq}}{[\mathrm{Enol\ 1D}]_{eq}}$$

Figure S4 Rate equations and boundary conditions of mechanism 2.

doi:10.6342/NTU202503041

Table S1 Conditions and results of base catalysis for AA tautomerization in CH_3CN.

Here, AA was added as vapor by a syringe. [AA] = 6.60×10^{-5} M; T = 25.1 ± 0.1°C

[TEA] / M	[H_2O] / M	k_{obs} / s^{-1}
1.64×10^{-5}	0	1.15×10^{-2}
	0.56	1.19×10^{-2}
	1.12	1.28×10^{-2}
	1.68	1.31×10^{-2}
	2.25	1.30×10^{-2}
4.22×10^{-5}	0	2.84×10^{-2}
	0.56	2.98×10^{-2}
	1.13	3.20×10^{-2}
	1.68	3.32×10^{-2}
	2.23	3.39×10^{-2}
8.88×10^{-5}	0	5.73×10^{-2}
	0.57	6.27×10^{-2}
	1.13	6.51×10^{-2}
	1.69	6.62×10^{-2}
	2.26	6.81×10^{-2}

doi:10.6342/NTU202503041

Table S2 Conditions and results of AA tautomerization in organic solvents mixed with water.

[AA] = 4.86×10^{-5} M; [HCL] = 3.39×10^{-4} M; T = 23.2°C.

MeOH/H_2O w/HCL		
Organic mole fraction, X_s	k_{obs} / s^{-1}	$Log_{10}(k_{obs}$ / $s^{-1})$
4.40×10^{-3}	1.07×10^{-1}	−0.97
0.13	8.26×10^{-2}	−1.08
0.30	4.72×10^{-2}	−1.33
0.55	1.90×10^{-2}	−1.72
0.69	1.06×10^{-2}	−1.98
0.86	3.86×10^{-3}	−2.41
0.96	1.19×10^{-3}	−2.92
EtOH/H_2O w/HCL		
Organic mole fraction, X_s	k_{obs} / s^{-1}	$Log_{10}(k_{obs}$ / $s^{-1})$
3.05×10^{-3}	1.13×10^{-1}	−0.95
9.11×10^{-2}	9.29×10^{-2}	−1.03
0.23	4.49×10^{-2}	−1.35
0.35	3.09×10^{-2}	−1.51
0.46	2.57×10^{-2}	−1.59
0.61	1.81×10^{-2}	−1.74
0.81	8.23×10^{-3}	−2.08
0.94	2.38×10^{-3}	−2.62

doi:10.6342/NTU202503041

Table S2 Continued

CH_3CN/H_2O		
Organic mole fraction, X_s	k_{obs} / s^{-1}	$Log_{10}(k_{obs} / s^{-1})$
3.44×10^{-3}	9.87×10^{-2}	−1.00
0.10	3.82×10^{-2}	−1.42
0.11	3.86×10^{-2}	−1.41
0.25	9.54×10^{-3}	−2.02
0.26	9.46×10^{-3}	−2.02
0.50	2.08×10^{-3}	−2.68
0.51	1.83×10^{-3}	−2.74
0.74	2.48×10^{-4}	−3.61
0.76	2.10×10^{-4}	−3.68
0.93	6.84×10^{-5}	−4.16
CD_3CN/D_2O		
Organic mole fraction, X_s	[a]k_{obs} / s^{-1}	$Log_{10}(k_{obs} / s^{-1})$
0	3.74×10^{-3}	−2.43
0	3.65×10^{-3}	−2.44
0.10	1.51×10^{-3}	−2.82
0.26	4.36×10^{-4}	−3.36
0.51	9.48×10^{-5}	−4.02

a. k_{obs} were obtained by fitting first-order kinetics (E5) of enol 6H

doi:10.6342/NTU202503041

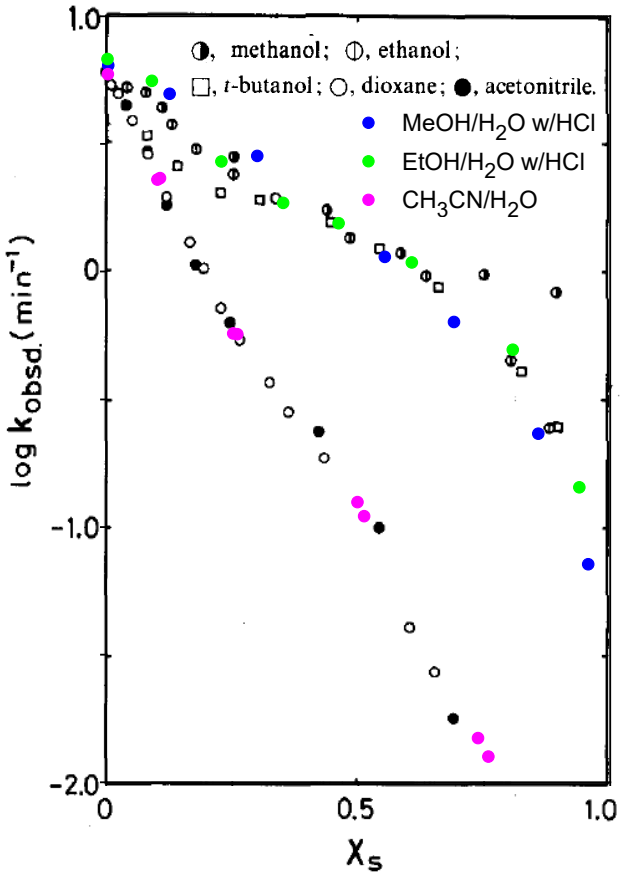

Figure S5 Comparison of plots of $Log_{10}(k_{obs}$ / $min^{-1})$ against X_s between the work of Watarai *et al.*[12] (black dots) and this work (colored dots).

The colored data are the same as those in Figure 13 and Figure 14, but presented in different units. Some inconsistency between our data and those of Watarai *et al.* (especially for methanol) may be attributed to the effect of residual base.

doi:10.6342/NTU202503041

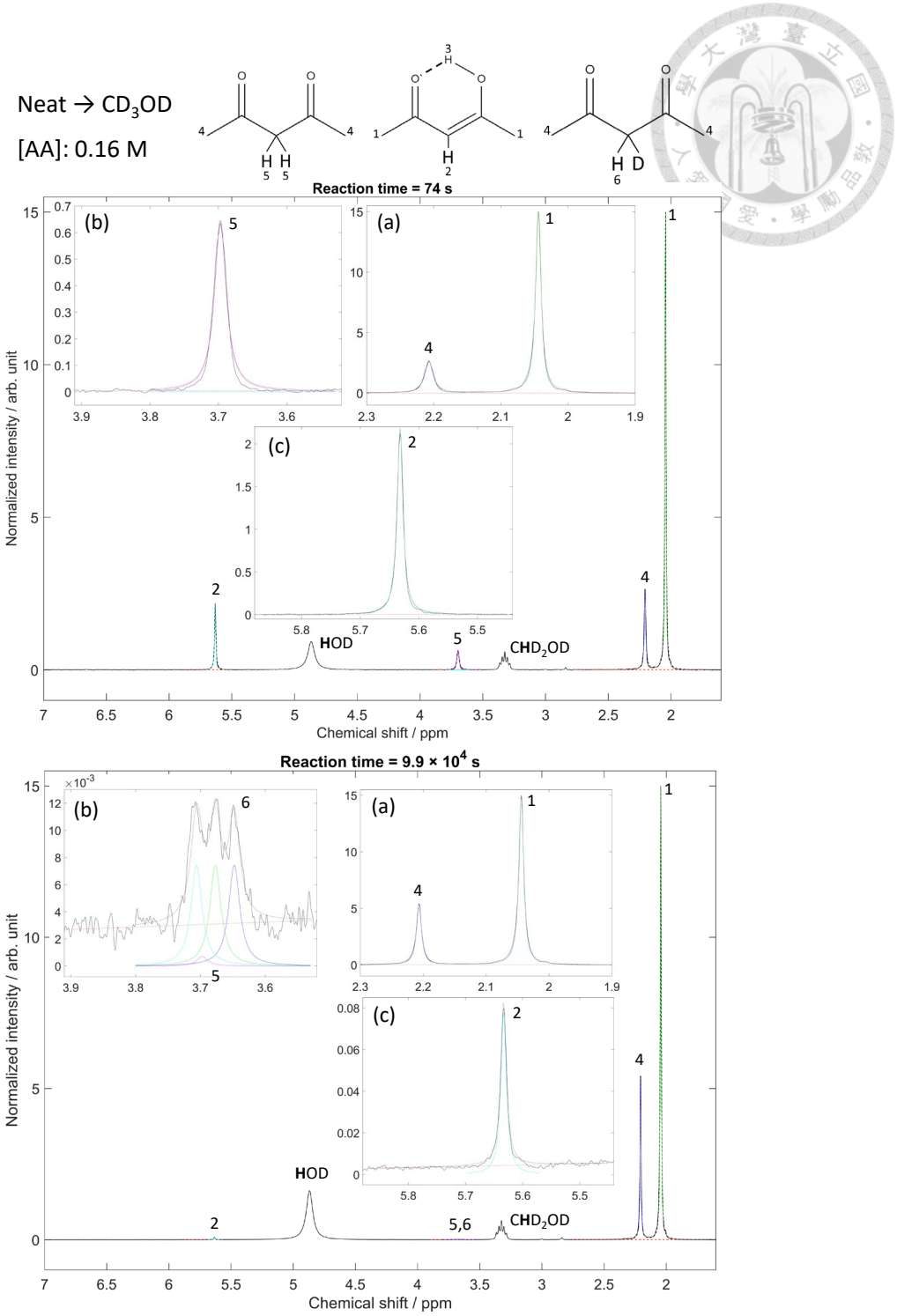

Figure S6 NMR spectrum of neat AA liquid in CD_3OD.

Experimental conditions: [AA]: 0.16 M, T = 25.0°C. Upper and lower panels are the spectrums at 74 and 9.9×10^4 s, respectively. The experiment was conducted at 80 MHz NMR, and peaks were referenced to enol 6H at 2.044 ppm. The red dashed lines are the linear baseline fits, and the colored lines are Lorentzian fits (E1).

doi:10.6342/NTU202503041

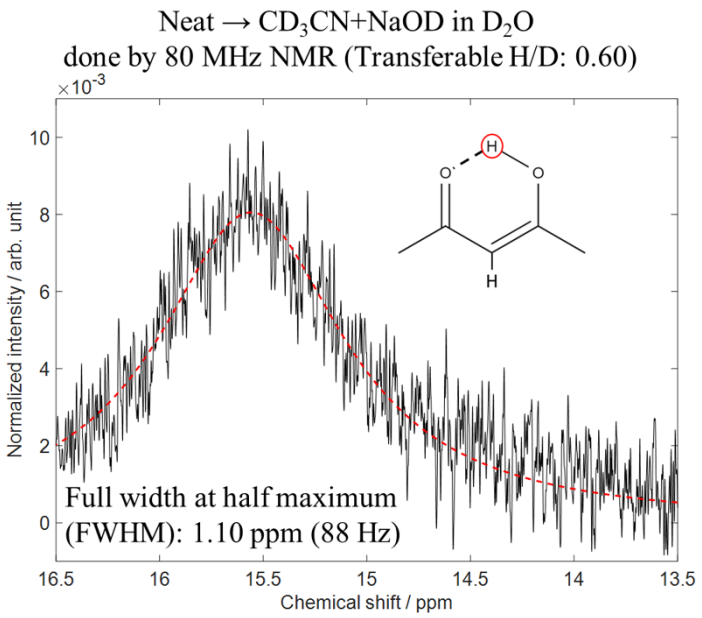

Figure S7 NMR spectrum of enol OH of neat AA in CD_3CN+NaOD in D_2O.

The experiment is conducted at 80 MHz NMR and the transferable H/D is ca. 0.60. The red line is the Lorentzian fit (E1), giving large FWHM of 88 Hz.

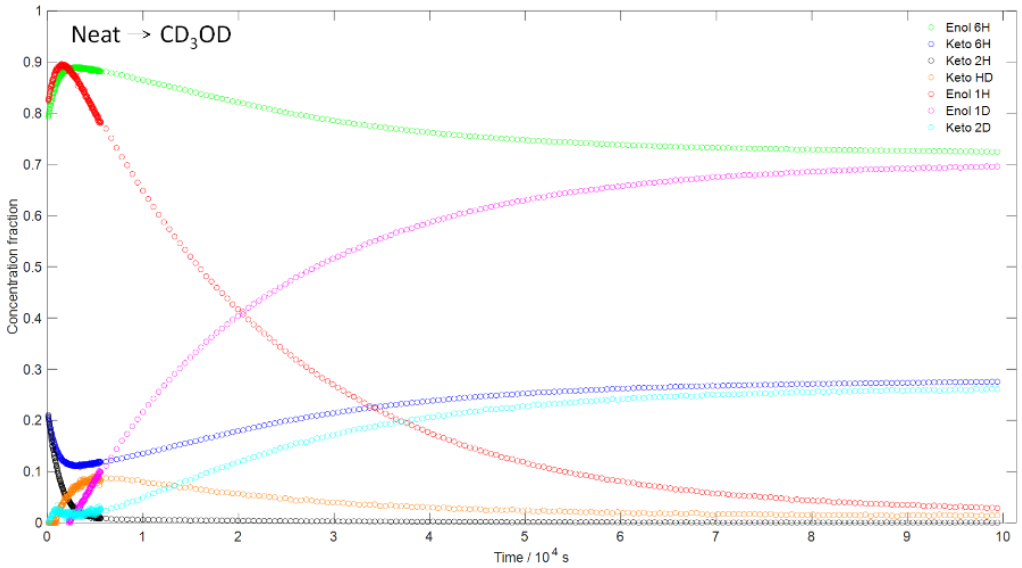

Figure S8 Raw data of time profiles of neat AA tautomerization in CD_3OD.

Experimental conditions: [AA]: 0.16 M, T = 25.0°C. The experiment was conducted at 80 MHz NMR. Hollow circles are measured concentration fractions of corresponding AA peaks. Enol 1D (magenta) and keto 2D (cyan) are calculated from (E13) and (E14), respectively.

doi:10.6342/NTU202503041

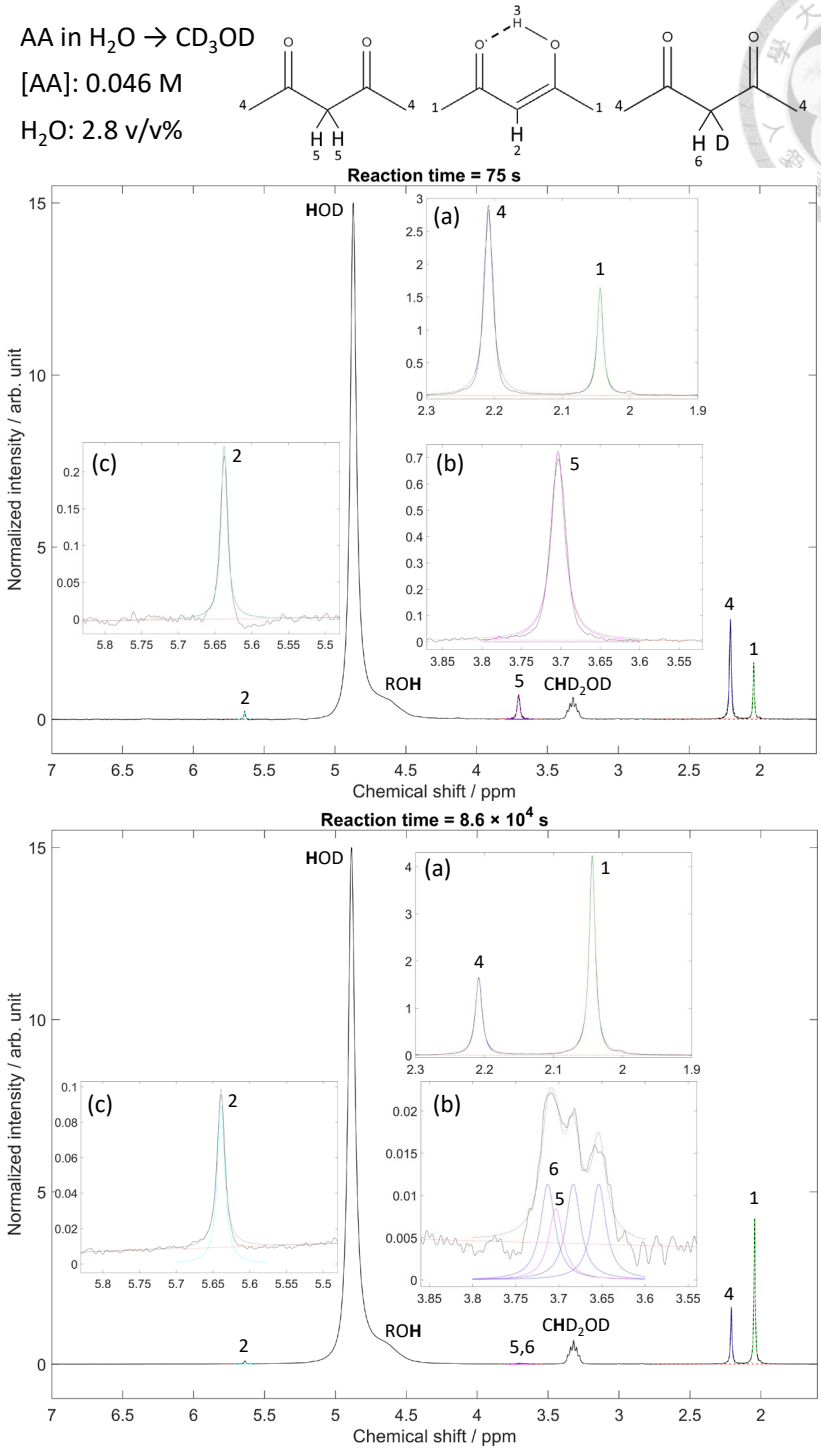

Figure S9 NMR spectrum of AA in $H_2O \rightarrow CD_3OD$.

Experimental conditions: [AA]: 0.046 M, T = 25.0°C. Upper and lower panels are the spectrums at 75 and 8.6×10^4 s, respectively. The experiment was conducted at 80 MHz NMR, and peaks were referenced to enol 6H at 2.044 ppm. The red dashed lines are the linear baseline fits, and the colored lines are Lorentzian fits (E1).

doi:10.6342/NTU202503041

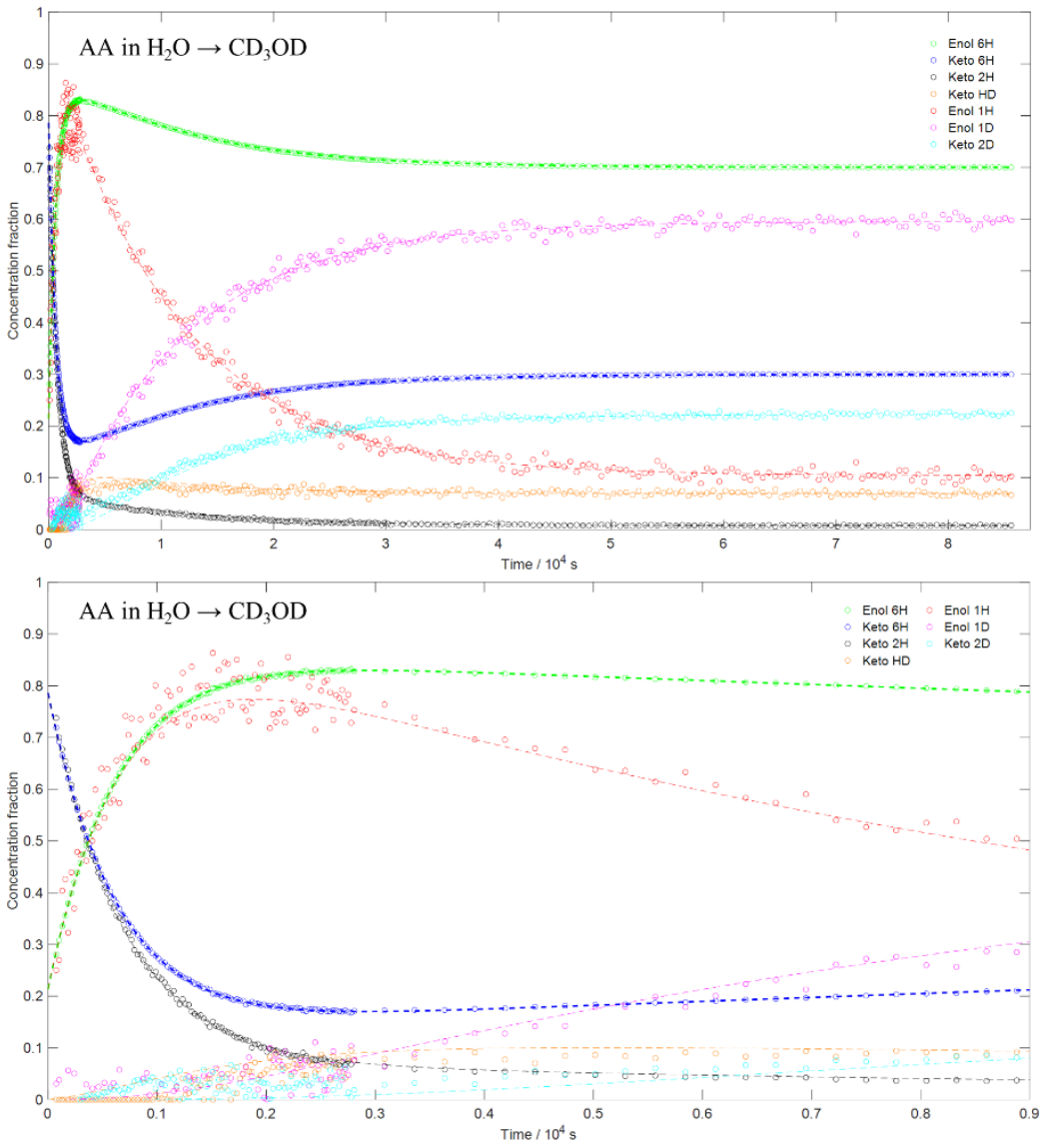

Figure S10 Time profiles (upper panel) and the enlarge (lower panel) of AA in H_2O → CD_3OD.

Experimental conditions: [AA]: 0.046 M; T = 25.0°C; ns: 1 for first 100 points, 10 for the following 100 points, and 20 for the last 100 points. The results are summarized as Exp #3 in Table 5. The meanings of data points and curves are the same as those described in Figure 17.

doi:10.6342/NTU202503041

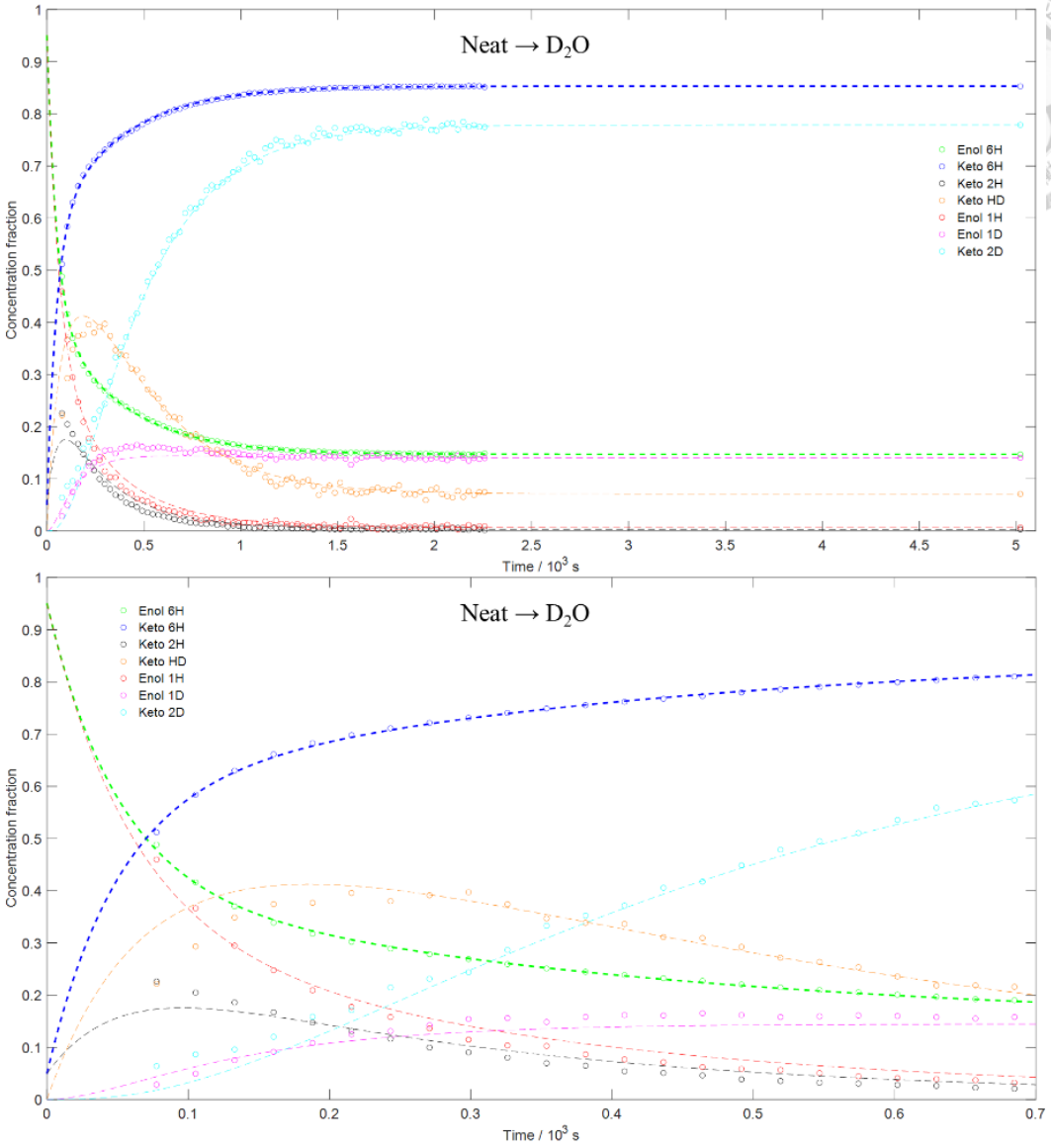

Figure S11 Time profiles (upper panel) and the enlarge (lower panel) of neat AA tautomerization in D_2O.

Experimental conditions: [AA]: 0.32 M; T = 25.0°C; ns: 1 for first 80 points and 100 for the last point. The results are summarized as Exp #1 in Table 5. The meanings of data points and curves are the same as those described in Figure 17.

doi:10.6342/NTU202503041

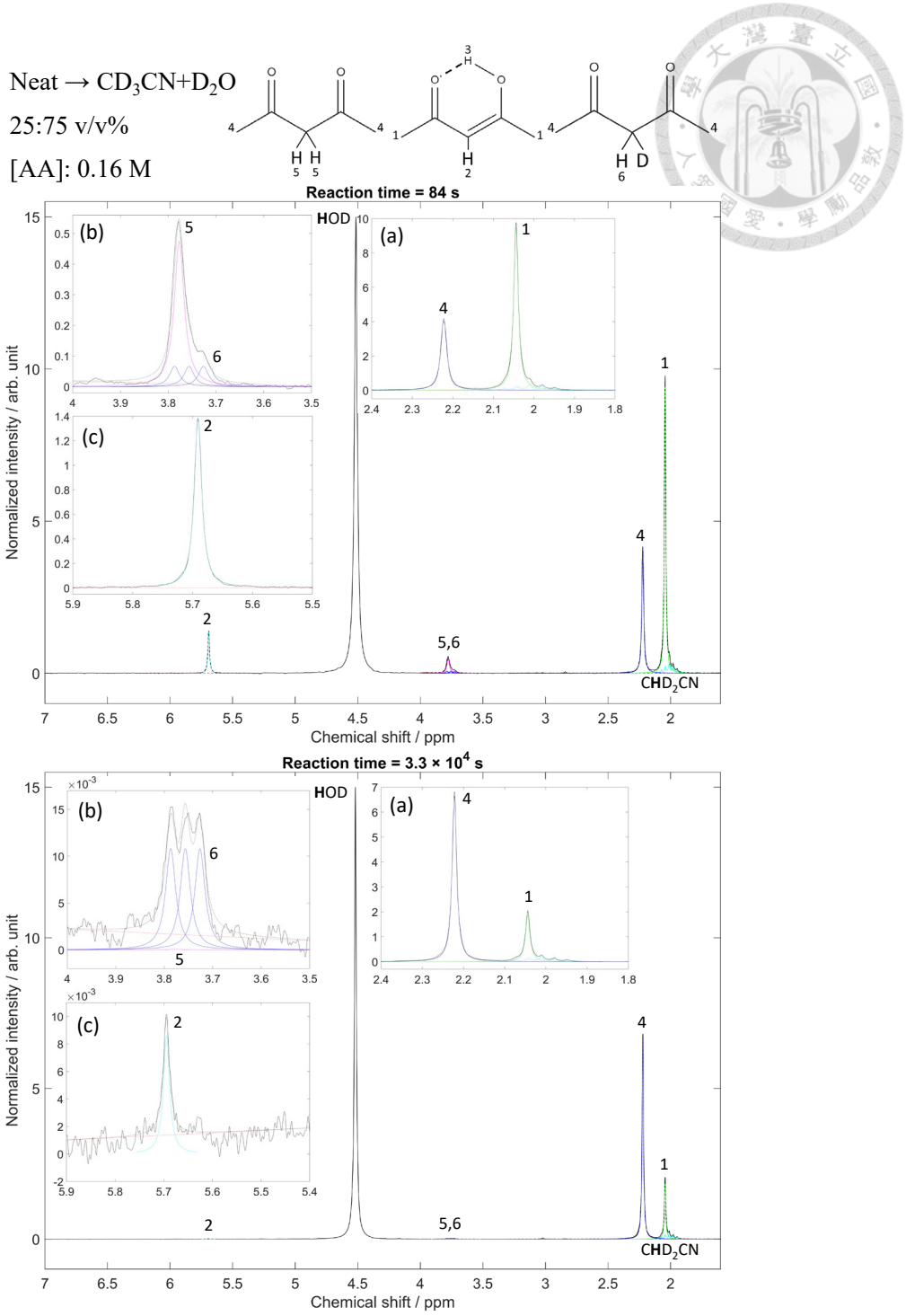

Figure S12 NMR spectrum of neat AA in CD_3CN/D_2O, 25:75 v/v%.

Experimental conditions: [AA]: 0.16 M; [D_2O]: 40.9 M; T = 25.0°C. Upper and lower panels are the spectrums at 84 and 3.3×10^4 s, respectively. The experiment was conducted at 80 MHz NMR, and peaks were referenced to enol 6H at 2.044 ppm. The red dashed lines are the linear baseline fits, and the colored lines are Lorentzian fits (E1).

doi:10.6342/NTU202503041

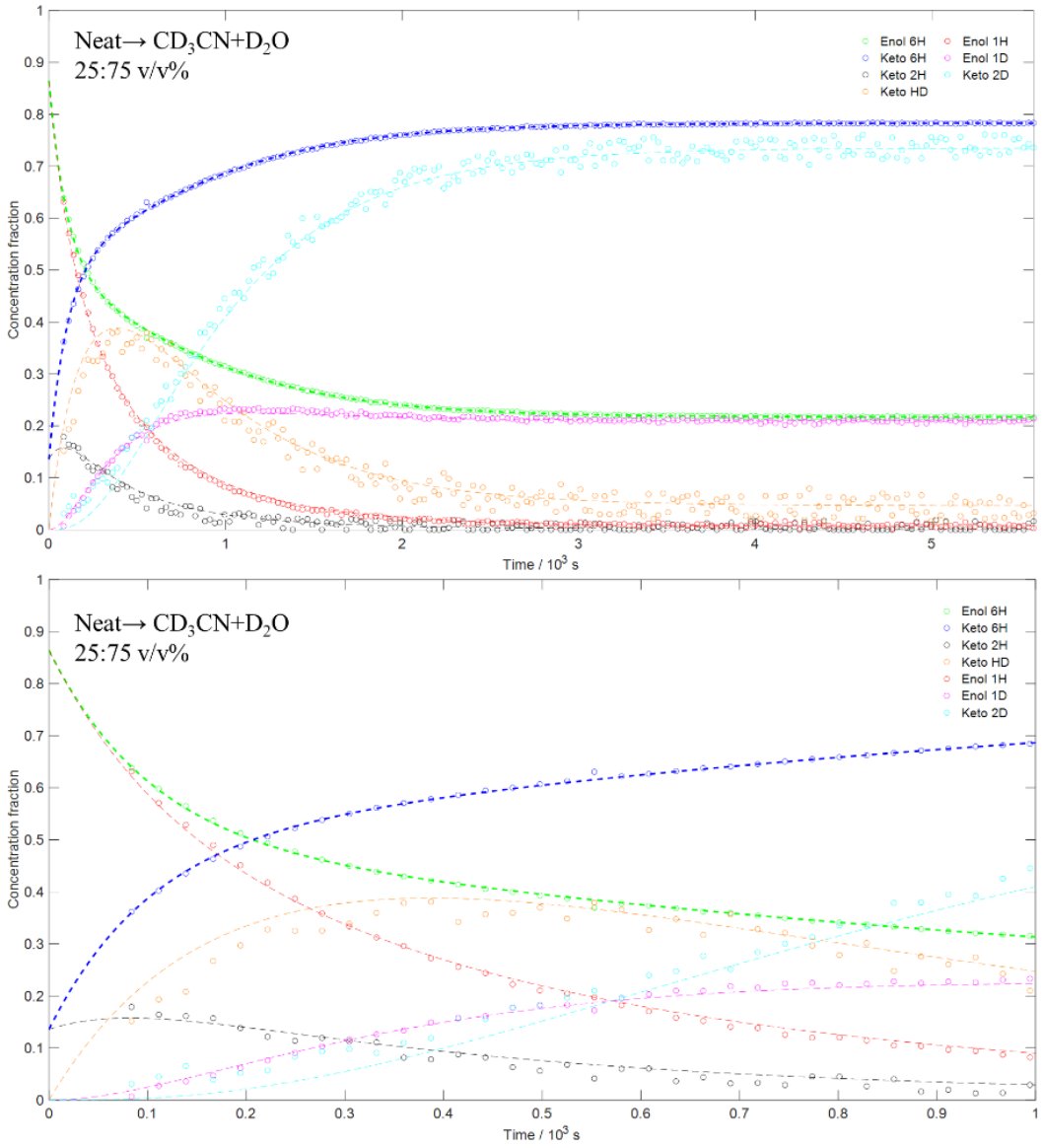

Figure S13 Time profiles (upper panel) and the enlarge (lower panel) of neat AA in CD_3CN/D_2O, 25:75 v/v%.

Experimental conditions: [AA]: 0.16 M; [D_2O]: 40.9 M; T = 25.0°C; ns: 1. The results are summarized as Exp #4 in Table 6. The meanings of data points and curves are the same as those described in Figure 17.

doi:10.6342/NTU202503041

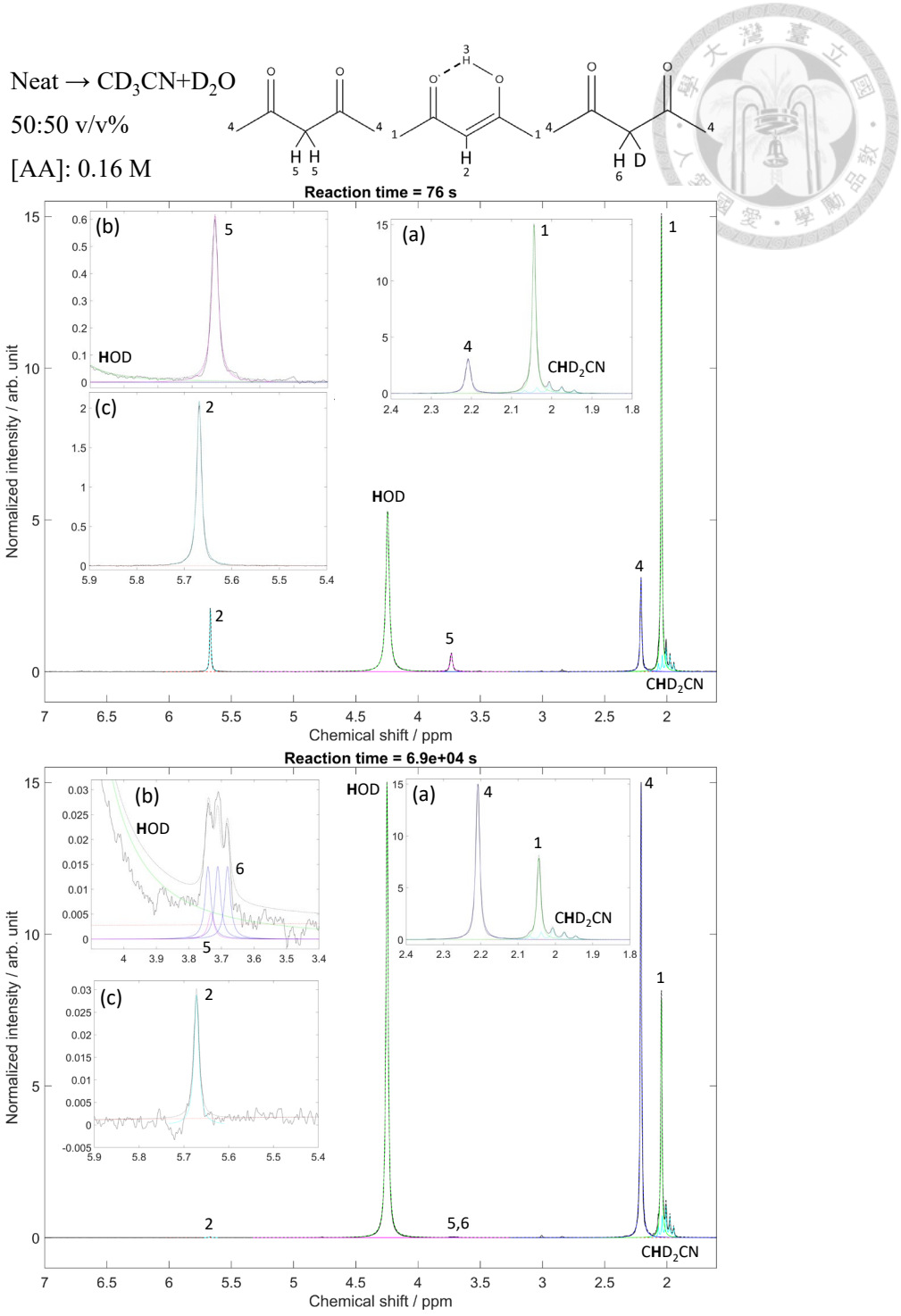

Figure S14 NMR spectrum of neat AA in CD_3CN/D_2O, 50:50 v/v%.

Experimental conditions: [AA]: 0.16 M; [D_2O]: 27.3 M; T = 25.0°C. Upper and lower panels are the spectrums at 76 and 6.9×10^4 s, respectively. The experiment was conducted at 80 MHz NMR, and peaks were referenced to enol 6H at 2.044 ppm. The red dashed lines are the linear baseline fits, and the colored lines are Lorentzian fits (E1).

doi:10.6342/NTU202503041

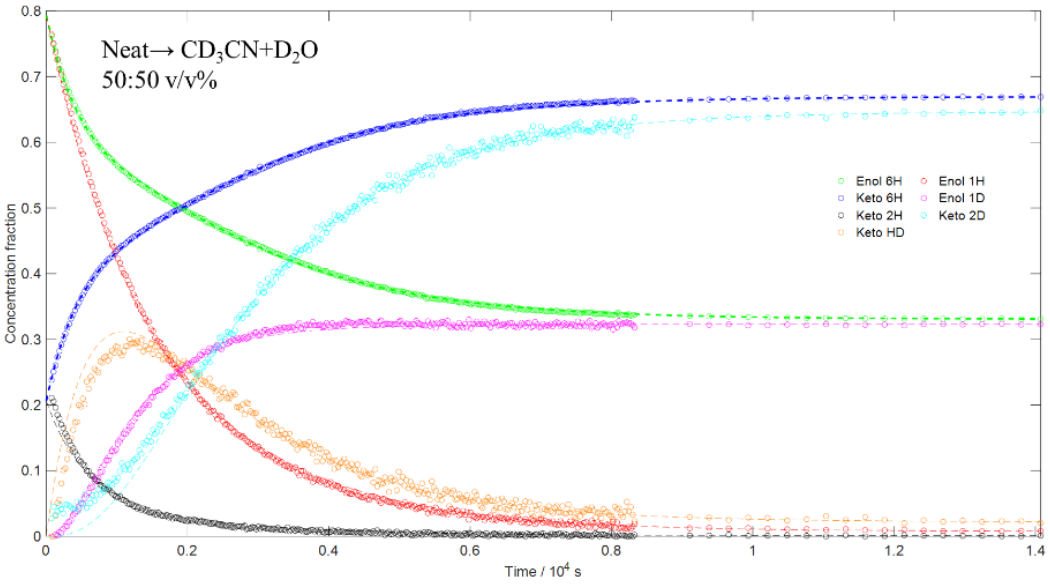

Figure S15 Time profiles of neat AA in CD_3CN/D_2O, 50:50 v/v%.

Experimental conditions: [AA]: 0.16 M; [D_2O]: 27.3 M; T = 25.0°C; ns: 1 for first 300 points, 10 for the others. The results are summarized as Exp #5 in Table 6. The meanings of data points and curves are the same as those described in Figure 17. Note that the initial fraction of enol 1H was revised, as its fraction was approximately 2% higher than that of enol 6H, complicating the model simulation.

doi:10.6342/NTU202503041

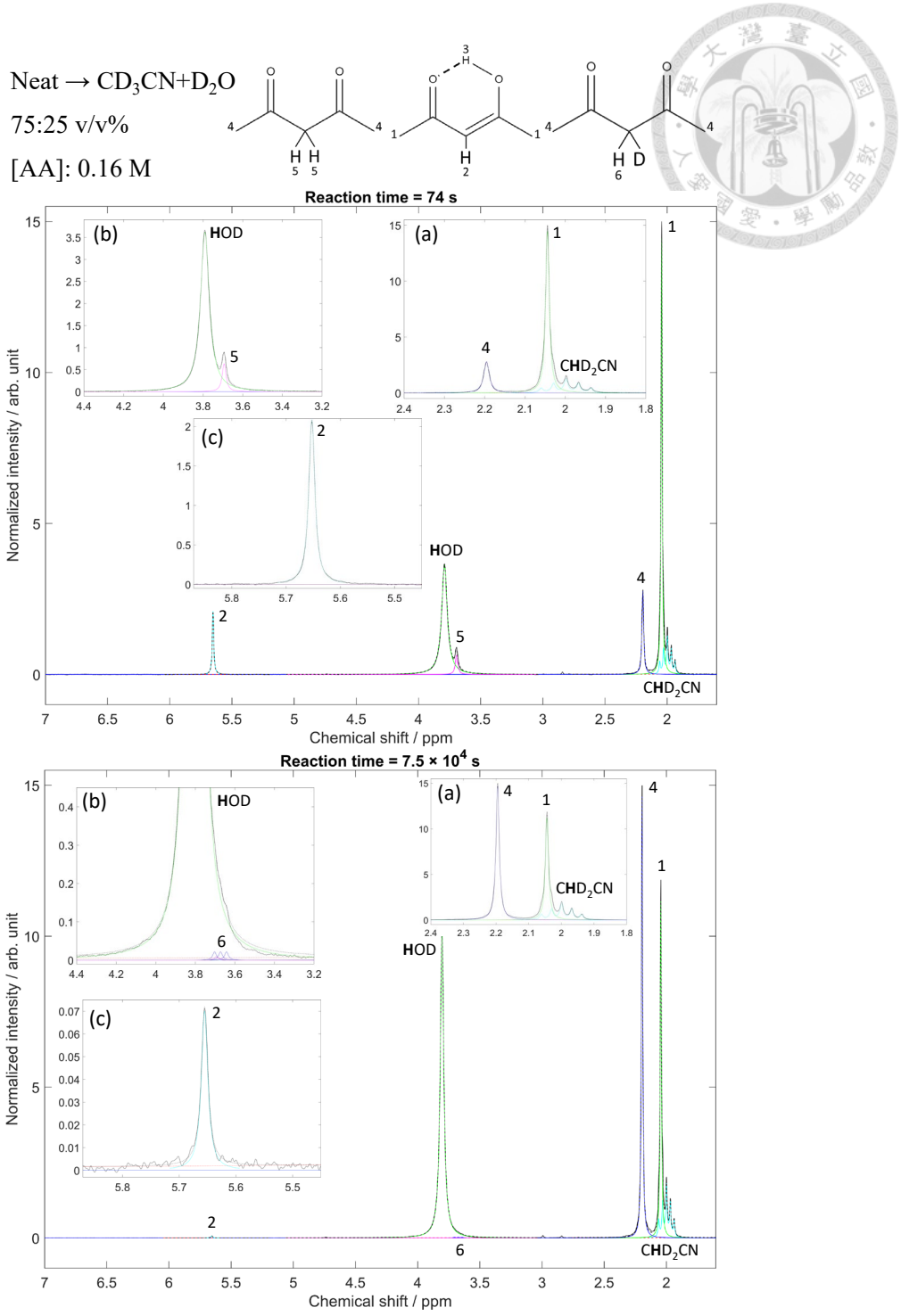

Figure S16 NMR spectrum of neat AA in CD_3CN/D_2O, 75:25 v/v%.

Experimental conditions: [AA]: 0.16 M; [D_2O]: 13.6 M; T = 25.0°C. Upper and lower panels are the spectrums at 74 and 7.5×10^4 s, respectively. The experiment was conducted at 80 MHz NMR, and peaks were referenced to enol 6H at 2.044 ppm. The red dashed lines are the linear baseline fits, and the colored lines are Lorentzian fits (E1).

doi:10.6342/NTU202503041

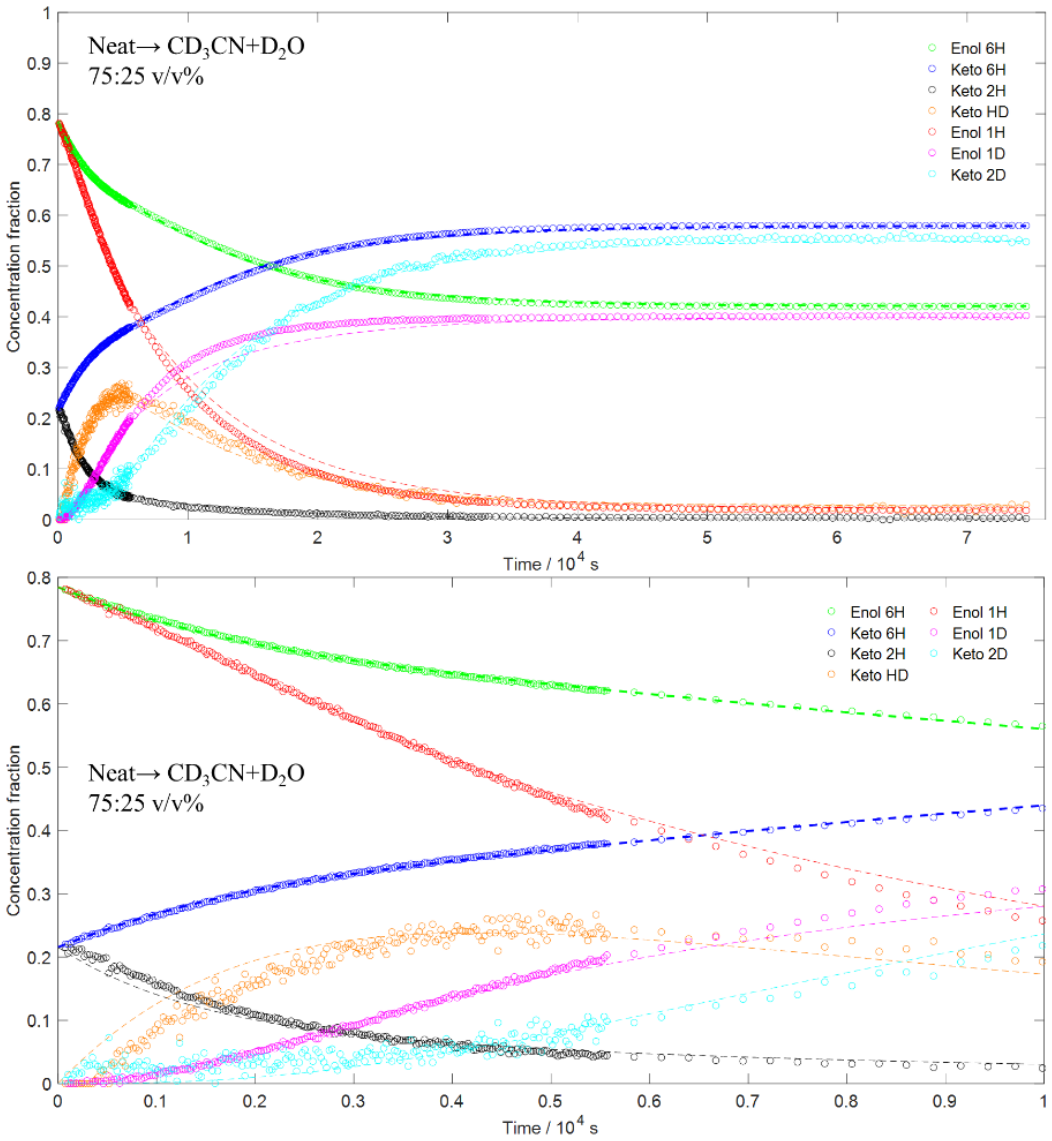

Figure S17 Time profiles of neat AA in CD_3CN/D_2O, 75:25 v/v%.

Experimental conditions: [AA]: 0.16 M; [D_2O]: 13.6 M; T = 25.0°C; ns: 1 for first 200 points, 10 for the following 100 points, and 20 for the last 75 points. The results are summarized as Exp #6 in Table 6. The meanings of data points and curves are the same as those described in Figure 17. Note that the initial fraction of enol 1H was revised, as its fraction was approximately 5% higher than that of enol 6H, complicating the model simulation.

doi:10.6342/NTU202503041

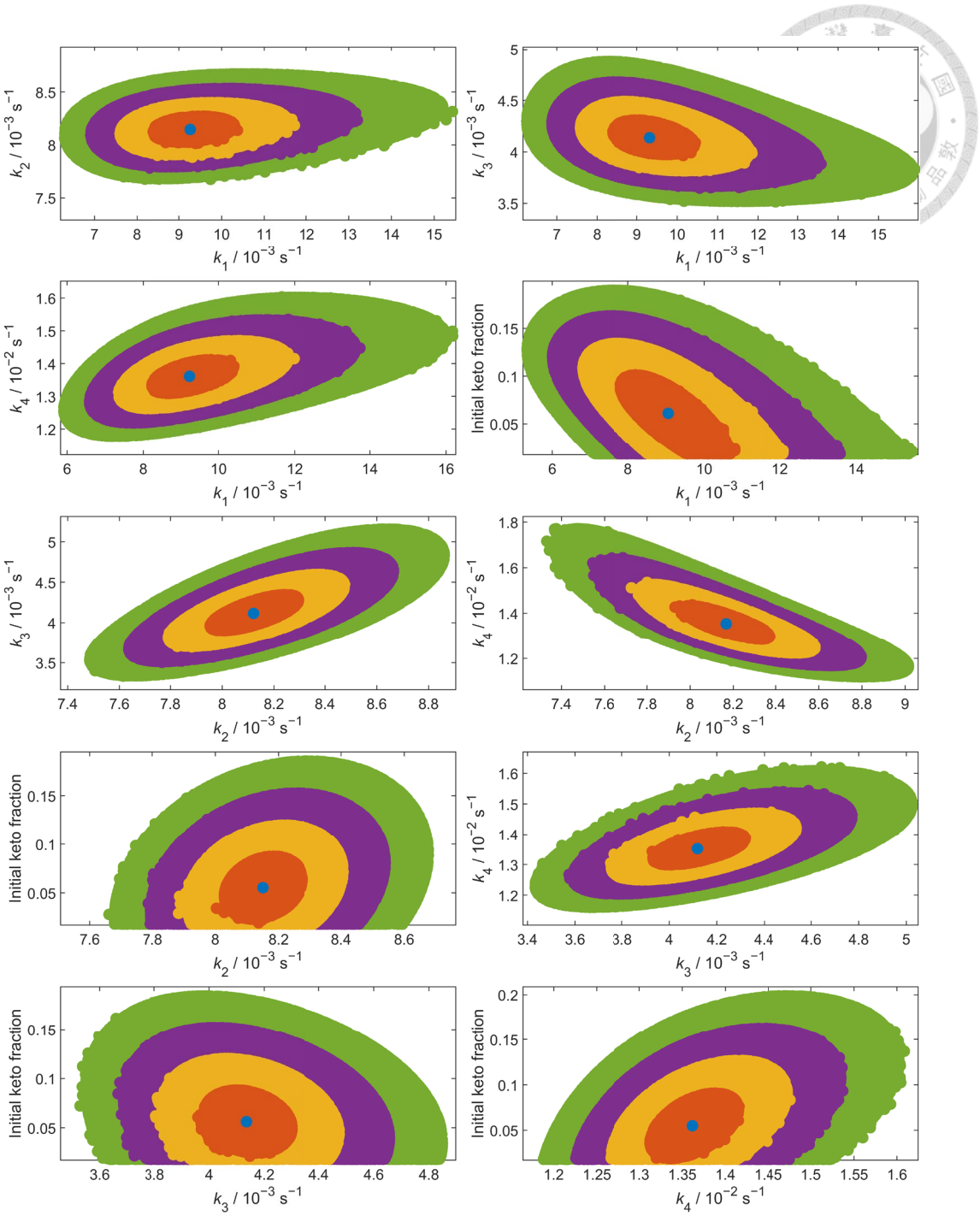

Figure S18 Fits of two variables in Exp #1.

The remaining variables were fixed at the values obtained from global fits, as shown in Table 5. The blue, orange, yellow, purple, and green points correspond to errors of 0, 0.25, 0.5, 0.75, and 1 SD, respectively.

doi:10.6342/NTU202503041

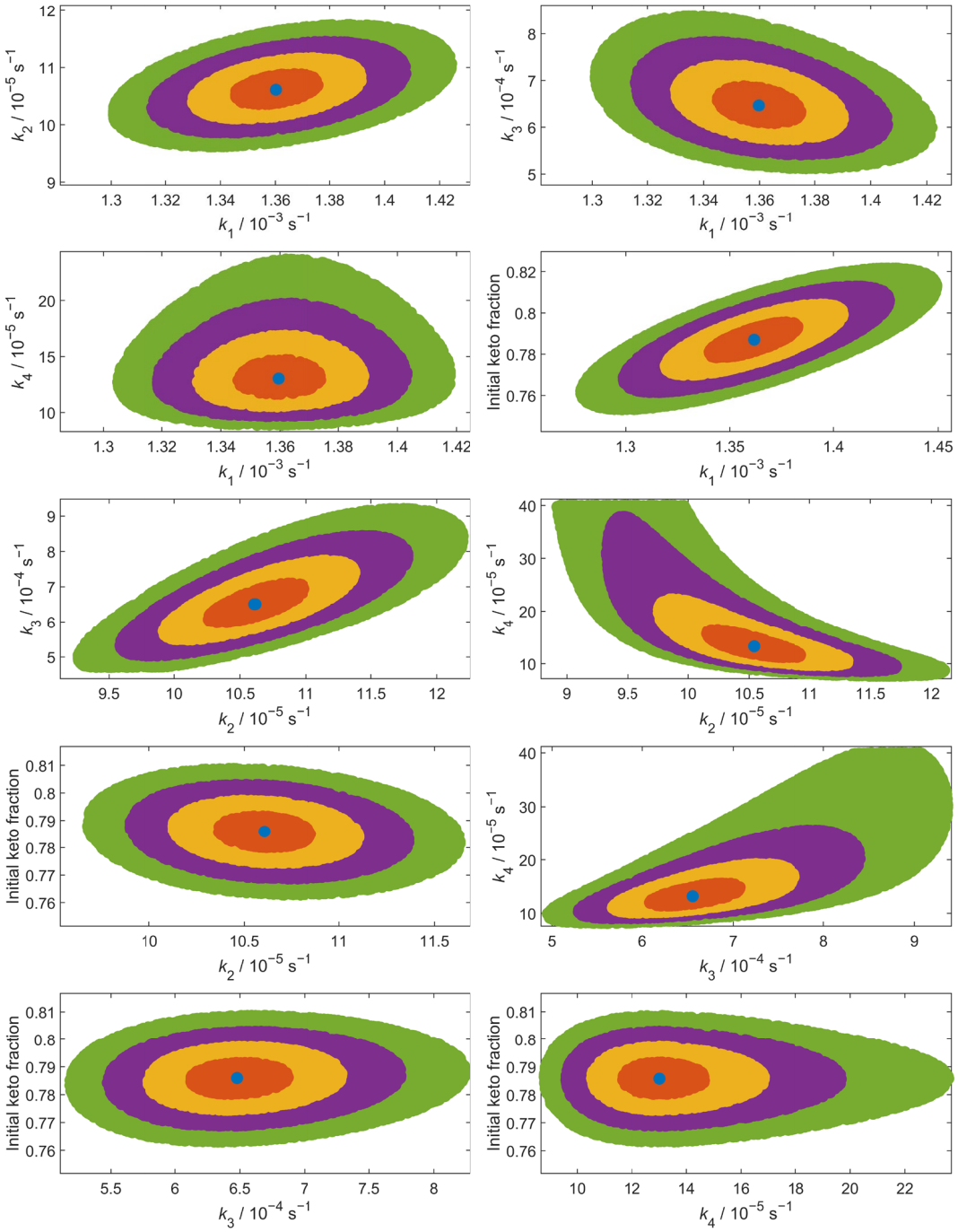

Figure S19 Fits of two variables in Exp #3

The remaining variables were fixed at the values obtained from global fits, as shown in Table 5. The blue, orange, yellow, purple, and green points correspond to errors of 0, 0.25, 0.5, 0.75, and 1 SD, respectively.

doi:10.6342/NTU202503041

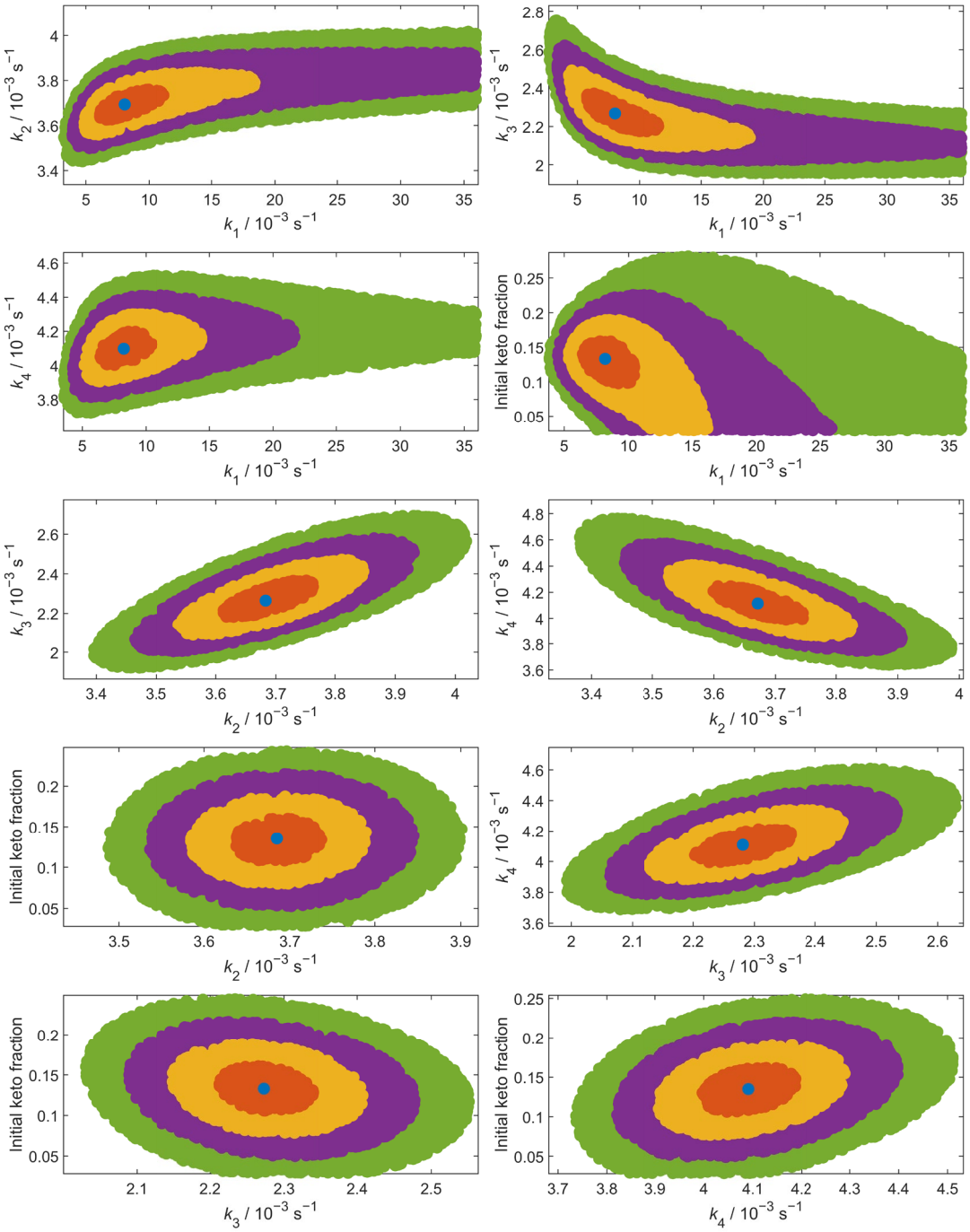

Figure S20 Fits of two variables in Exp #4

The remaining variables were fixed at the values obtained from global fits, as shown in Table 6. The blue, orange, yellow, purple, and green points correspond to errors of 0, 0.25, 0.5, 0.75, and 1 SD, respectively.

doi:10.6342/NTU202503041

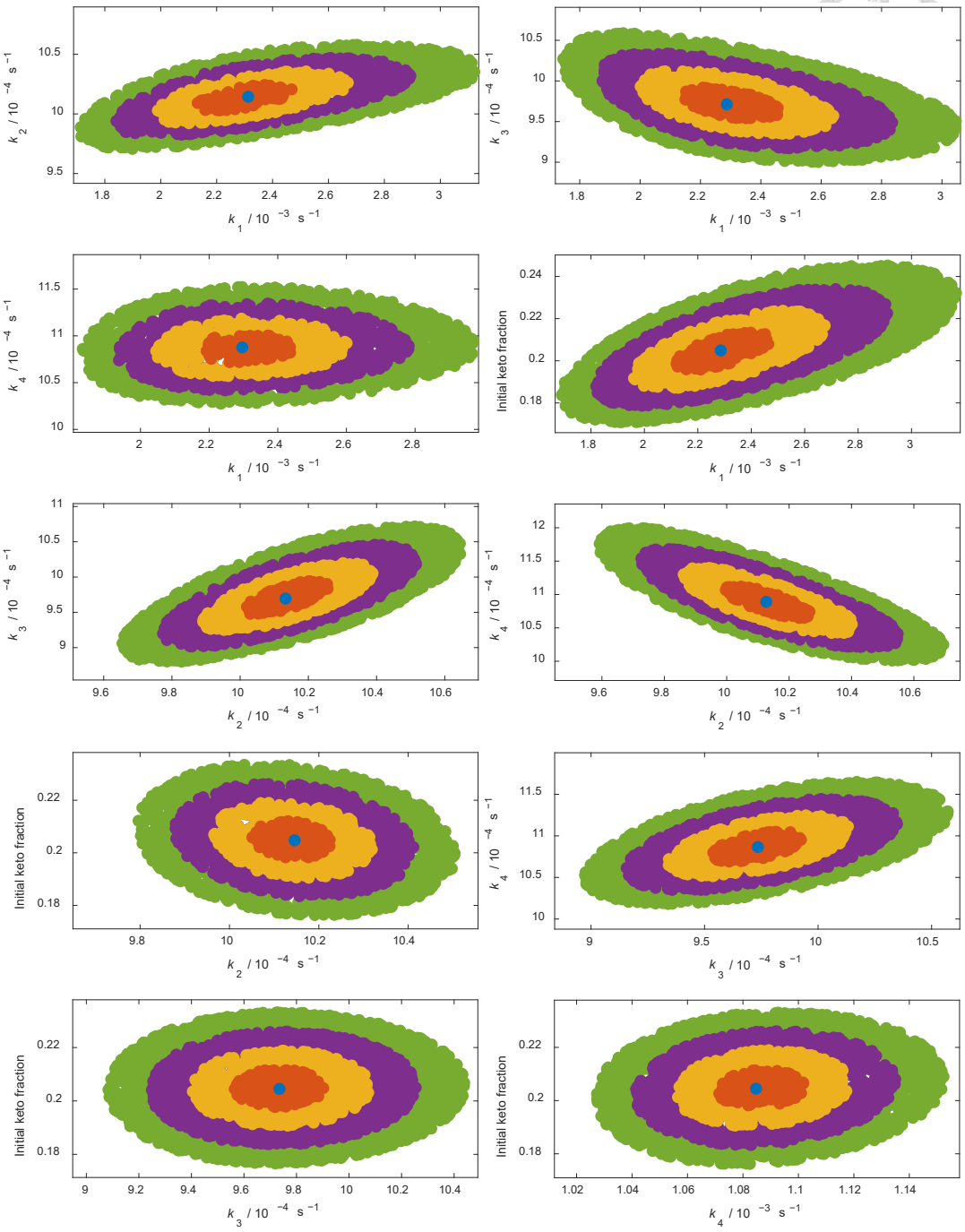

Figure S21 Fits of two variables in Exp #5

The remaining variables were fixed at the values obtained from global fits, as shown in Table 6. The blue, orange, yellow, purple, and green points correspond to errors of 0, 0.25, 0.5, 0.75, and 1 SD, respectively.

doi:10.6342/NTU202503041

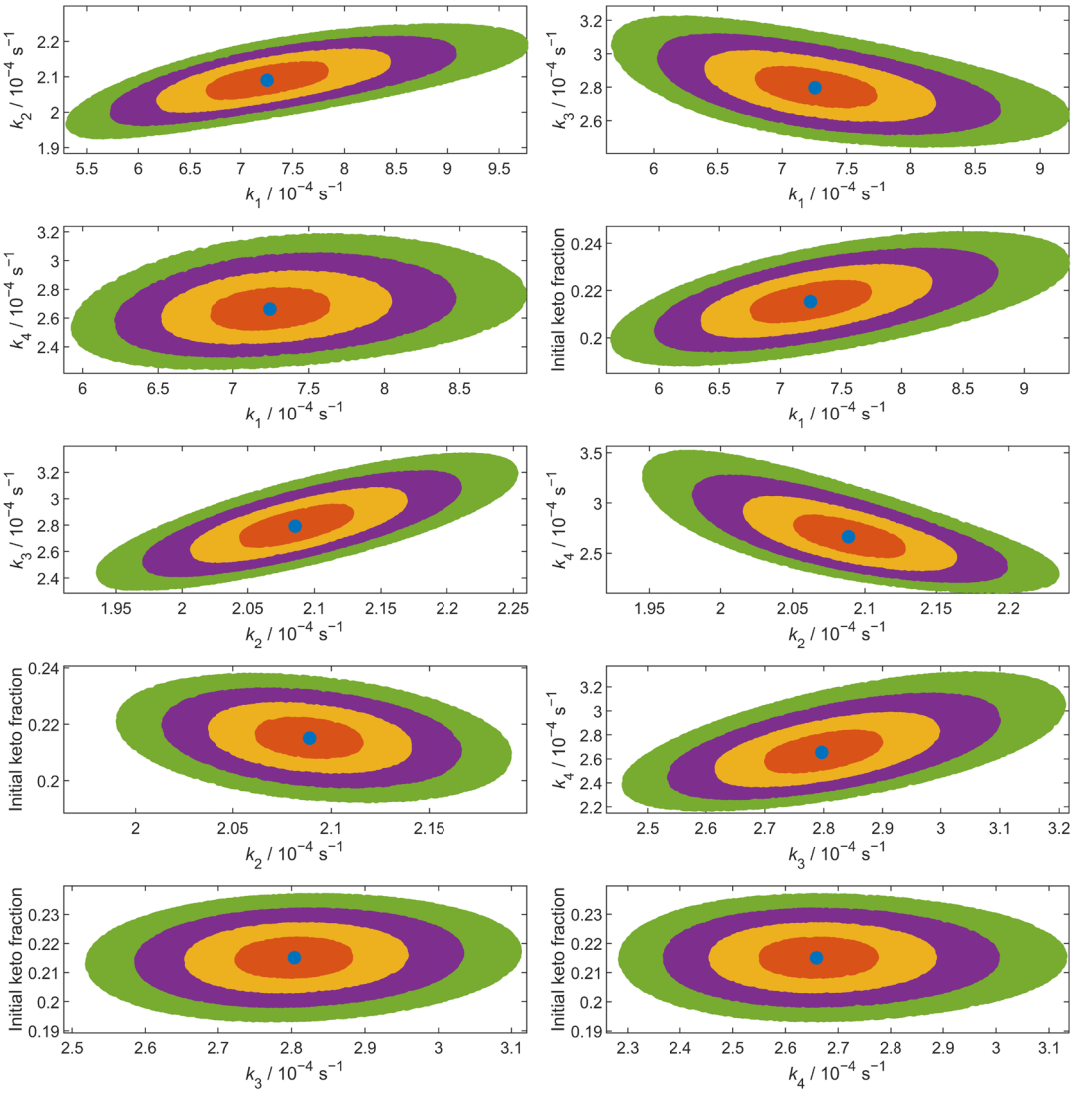

Figure S22 Fits of two variables in Exp #6

The remaining variables were fixed at the values obtained from global fits, as shown in Table 6. The blue, orange, yellow, purple, and green points correspond to errors of 0, 0.25, 0.5, 0.75, and 1 SD, respectively.

doi:10.6342/NTU202503041

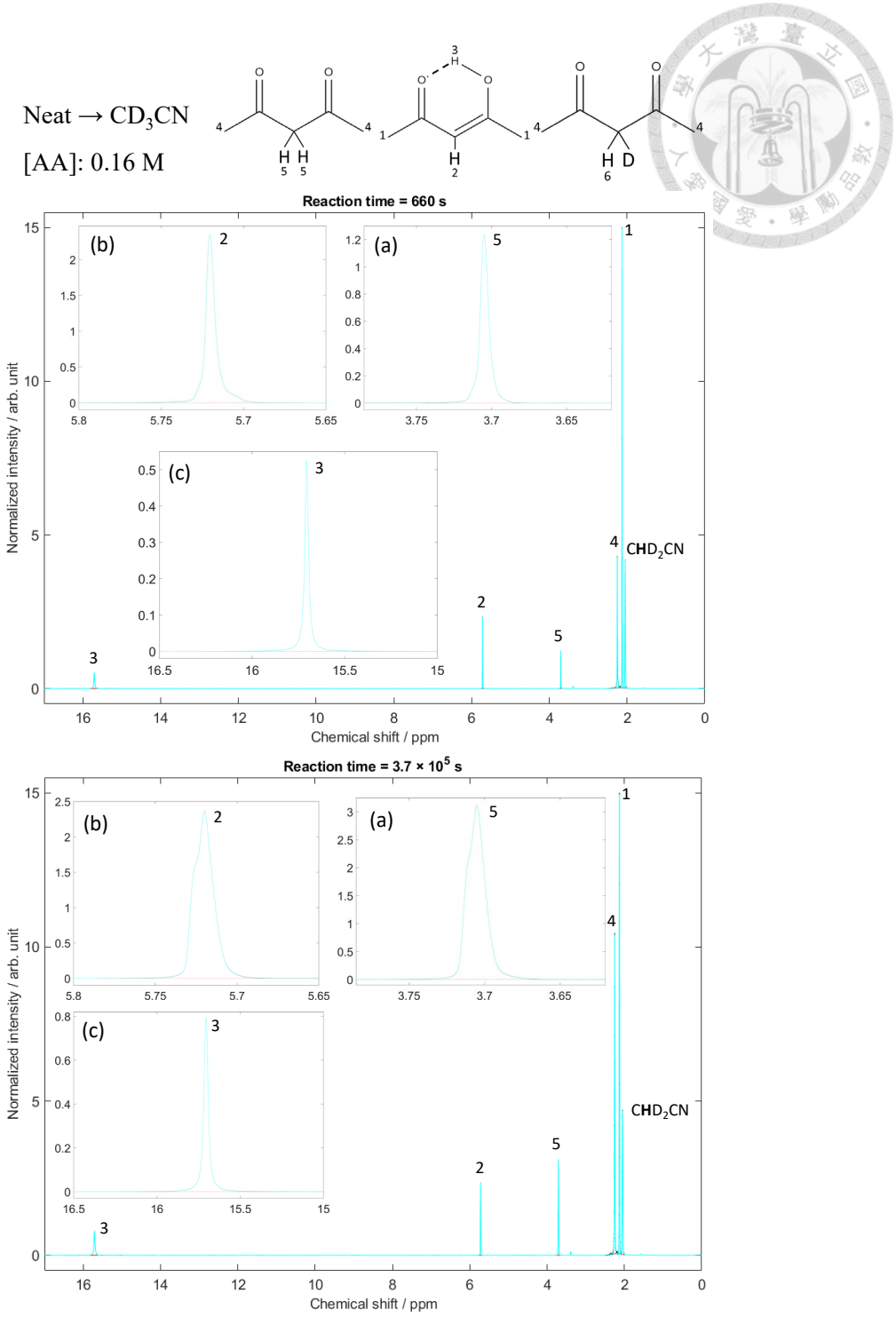

Figure S23 NMR spectrum of neat AA in CD_3CN.

Experimental conditions: [AA]: 0.16 M; T = 25.0°C. Upper and lower panels are the spectrums at 660 and 3.7×10^5 s, respectively. The red dashed lines are the linear baseline fits. The experiment was conducted at 600 MHz NMR, and peaks were integrated between the chemical shifts corresponding to one percent of the peak's maxima intensity.

doi:10.6342/NTU202503041

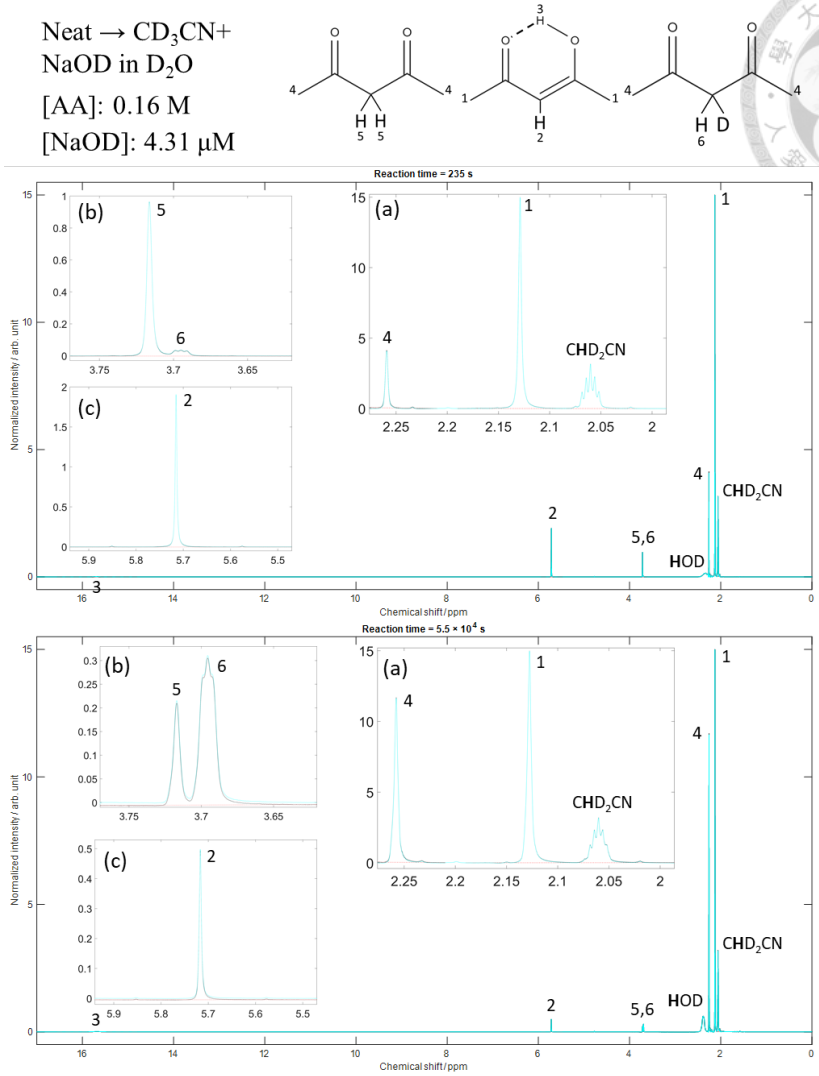

Figure S24 NMR spectrum of neat AA in CD_3CN+NaOD in D_2O.

Experimental conditions: [AA]: 0.16 M; [NaOD]: 4.31×10^{-6} M; [D_2O]: 0.54 M; T = 25.0°C. Upper and lower panels are the spectrums at 235 and 5.5×10^4 s, respectively. The red dashed lines are the linear baseline fits. The experiment was conducted at 600 MHz NMR, and peaks were integrated between the chemical shifts corresponding to one percent of the peak's maxima intensity.

doi:10.6342/NTU202503041

REFERENCE

(1) Hamaguchi, T.; Ono, K.; Yamada, M. Curcumin and Alzheimer's disease. *CNS Neurosci. Ther.* **2010**, *16* (5), 285-297.

(2) Kockler, J.; Robertson, S.; Oelgemöller, M.; Davies, M.; Bowden, B.; Brittain, H. G.; Glass, B. D. Butyl methoxy dibenzoylmethane. *Profiles of Drug Substances, Excipients and Related Methodology* **2013**, *38*, 87-111.

(3) Podyachev, S.; Sudakova, S.; Galiev, A.; Mustafina, A.; Syakaev, V.; Shagidullin, R.; Bauer, I.; Konovalov, A. Synthesis of tris (β-diketones) and study of their complexation with some transition metals. *Russ. Chem. Bull.* **2006**, *55*, 2000-2007.

(4) Meany, J. E. Reversible tautomerization of acetylacetone enol. I. Metal ion catalysis. *The Journal of Physical Chemistry* **1969**, *73* (10), 3421-3423.

(5) Radzyminska-Lenarcik, E.; Witt, K. The application of acetylacetone for the separation of heavy metals in roadside soil belts by extraction methods. *Desalination and Water Treatment* **2020**, *186*, 191-198.

(6) Sodhi, R. K.; Paul, S. An overview of metal acetylacetonates: Developing areas/routes to new materials and applications in organic syntheses. *Catalysis surveys from Asia* **2018**, *22*, 31-62.

(7) Glukhacheva, V. S.; Il'yasov, S. G.; Kazantsev, I. V.; Shestakova, E. O.; Il'yasov, D. S.; Eltsov, I. V.; Nefedov, A. A.; Gatilov, Y. V. New reaction products of acetylacetone with semicarbazide derivatives. *ACS omega* **2021**, *6* (12), 8637-8645.

(8) Eidinoff, M. L. Dissociation constants of acetylacetone, ethyl acetoacetate and benzoylacetone. *J. Am. Chem. Soc.* **1945**, *67* (12), 2072-2073.

(9) Bruice, P. Y. Role of the acidity of the ketone in determining the mechanism of enolization via proton abstraction from ketone, carbinolamine, or imine. Catalysis of the enolization of 2, 4-pentanedione and 3-methyl-2, 4-pentanedione by oxyanions and by primary, secondary, and tertiary amines. *J. Am. Chem. Soc.* **1990**, *112* (20), 7361-7368.

(10) Zhang, C.; Zhang, G.; Zheng, H.; Zhang, S. The Interplay of Hydration and Hydrolysis upon the Keto–Enol Tautomerism of β-Diketones. *J. Chem. Educ.* **2024**, *101*

doi:10.6342/NTU202503041

(12), 5460-5467.

(11) Messaadia, L.; El Dib, G.; Ferhati, A.; Chakir, A. UV–visible spectra and gas-phase rate coefficients for the reaction of 2, 3-pentanedione and 2, 4-pentanedione with OH radicals. *Chem. Phys. Lett.* **2015**, *626*, 73-79.

(12) Watarai, H.; Suzuki, N. Keto-enol tautomerization rates of acetylacetone in mixed aqueous media. *J. Inorg. Nucl. Chem.* **1974**, *36* (8), 1815-1820.

(13) Spyridis, G. T.; Meany, J. Tautomerization of acetylacetone enol: A physical organic experiment in kinetics and thermodynamics. *J. Chem. Educ.* **1988**, *65* (5), 461. DOI: 10.1021/ed065p461.

(14) Watarai, H.; Suzuki, N. Partition kinetic studies of acetylacetone: Base-catalysis in aqueous phase and solvent dependence. *J. Inorg. Nucl. Chem.* **1976**, *38* (2), 301-304.

(15) Watarai, H.; Suzuki, N. The base-catalyzed tautomerization of acetylacetone in organic solvents. The correlation of the catalytic coefficient with the partition coefficient. *Bull. Chem. Soc. Jpn.* **1979**, *52* (10), 2778-2782.

(16) Dawber, J. G.; Crane, M. M. Keto-enol tautomerization: A thermodynamic and kinetic study. *J. Chem. Educ.* **1967**, *44* (3), 150.

(17) Howard, D. L.; Kjaergaard, H. G.; Huang, J.; Meuwly, M. Infrared and near-infrared spectroscopy of acetylacetone and hexafluoroacetylacetone. *J. Phys. Chem. A* **2015**, *119* (29), 7980-7990.

(18) Reeves, L. Nuclear magnetic resonance measurements in solutions of acetylacetone: the effect of solvent interactions on the tautomeric equilibrium. *Can. J. Chem.* **1957**, *35* (11), 1351-1365.

(19) Sandusky, P. O. Expansion of the Classic Acetylacetone Physical Chemistry Laboratory NMR Experiment: Correlation of the Enol–Keto Equilibrium Position with the Solvent Dipole Moment. *J. Chem. Educ.* **2014**, *91* (5), 739-742.

(20) Manbeck, K. A.; Boaz, N. C.; Bair, N. C.; Sanders, A. M.; Marsh, A. L. Substituent effects on keto–enol equilibria using NMR spectroscopy. *J. Chem. Educ.* **2011**, *88* (10), 1444-1445.

(21) Schweitzer, G. K.; Benson, E. W. Enol content of some. beta.-diketones. *J. Chem. Eng. Data* **1968**, *13* (3), 452-453.

doi:10.6342/NTU202503041

(22) Nichols, M. A.; Waner, M. J. Kinetic and mechanistic studies of the deuterium exchange in classical keto−enol tautomeric equilibrium reactions. *J. Chem. Educ.* **2010**, *87* (9), 952-955.

(23) Mills, S. G.; Beak, P. Solvent effects on keto-enol equilibria: tests of quantitative models. *The Journal of Organic Chemistry* **1985**, *50* (8), 1216-1224.

(24) Maryott, A. A.; Smith, E. R. *Table of dielectric constants of pure liquids*; US Government Printing Office, 1951.

(25) Gregory, A.; Clarke, R. Traceable measurements of the static permittivity of dielectric reference liquids over the temperature range 5–50 C. *Meas. Sci. Technol.* **2005**, *16* (7), 1506.

(26) Watarai, H.; Suzuki, N. Keto-enol tautomerization rates of acetylacetone in water-acetonitrile and water-dimethyl sulfoxide mixtures: Rate-partition relationship. *J. Inorg. Nucl. Chem.* **1976**, *38* (9), 1683-1686.

(27) van Beek, J. D. matNMR: A flexible toolbox for processing, analyzing and visualizing magnetic resonance data in Matlab®. *J. Magn. Reson.* **2007**, *187* (1), 19-26.

(28) Petrakis, L. Spectral line shapes: Gaussian and Lorentzian functions in magnetic resonance. *J. Chem. Educ.* **1967**, *44* (8), 432.

(29) Voter, A. F. Introduction to the kinetic Monte Carlo method. In *Radiation effects in solids*, Springer, 2007; pp 1-23.

(30) Alagona, G.; Ghio, C.; Nagy, P. I. The catalytic effect of water on the keto–enol tautomerism. Pyruvate and acetylacetone: a computational challenge. *Physical Chemistry Chemical Physics* **2010**, *12* (35), 10173-10188.

(31) Yamabe, S.; Tsuchida, N.; Miyajima, K. Reaction paths of keto− enol tautomerization of β-diketones. *J. Phys. Chem. A* **2004**, *108* (14), 2750-2757.

(32) Delchev, V. B. Hydrogen bonded complexes of acetylacetone and methanol: HF and DFT level study. *Monatshefte für Chemie/Chemical Monthly* **2004**, *135*, 249-260.

(33) Schlund, S.; Basílio Janke, E. M.; Weisz, K.; Engels, B. Predicting the tautomeric equilibrium of acetylacetone in solution. I. The right answer for the wrong reason? *J. Comput. Chem.* **2010**, *31* (4), 665-670.

doi:10.6342/NTU202503041

(34) Agmon, N. The grotthuss mechanism. *Chem. Phys. Lett.* **1995**, *244* (5-6), 456-462.

(35) Rondinini, S.; Longhi, P.; Mussini, P.; Mussini, T. Autoprotolysis constants in nonaqueous solvents and aqueous organic solvent mixtures. *Pure and Applied Chemistry* **1987**, *59* (12), 1693-1702.

(36) Abrash, H. I. The relative acidities of water and methanol. *J. Chem. Educ.* **2001**, *78* (11), 1496.

(37) Bell, R. P. *Acids and Bases: Their Quantitative Behaviour*; Methuen, 1969.

(38) Williams, D. L. H.; Xia, L. Electrophilic substitution in malonamide. Evidence for reaction via the enol tautomer. *Journal of the Chemical Society, Perkin Transactions 2* **1993**, (8), 1429-1432.

(39) Toullec, J.; Dubois, J. Methylidyne-methylidyne-d and water-water-d2 isotope effects on the forward and reverse rates of keto-enol tautomerization of acetone in acidic media. *J. Am. Chem. Soc.* **1974**, *96* (11), 3524-3532.

doi:10.6342/NTU202503041